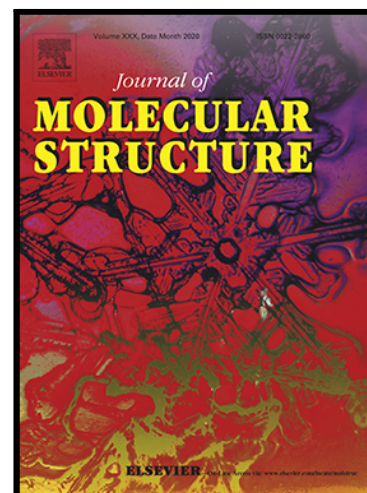


## Journal Pre-proof

Novel adamantane-pyrazole and hydrazone hybridized: design, synthesis, cytotoxic evaluation, SAR study and molecular docking simulation as carbonic anhydrase inhibitors

Mohammed M.S. Wassel , Ahmed Ragab , Gameel A.M. Elhag Ali , Ahmed B.M. Mehany , Yousry A. Ammar

PII: S0022-2860(20)31290-4  
DOI: <https://doi.org/10.1016/j.molstruc.2020.128966>  
Reference: MOLSTR 128966



To appear in: *Journal of Molecular Structure*

Received date: 26 June 2020  
Revised date: 23 July 2020  
Accepted date: 23 July 2020

Please cite this article as: Mohammed M.S. Wassel , Ahmed Ragab , Gameel A.M. Elhag Ali , Ahmed B.M. Mehany , Yousry A. Ammar , Novel adamantane-pyrazole and hydrazone hybridized: design, synthesis, cytotoxic evaluation, SAR study and molecular docking simulation as carbonic anhydrase inhibitors, *Journal of Molecular Structure* (2020), doi: <https://doi.org/10.1016/j.molstruc.2020.128966>

This is a PDF file of an article that has undergone enhancements after acceptance, such as the addition of a cover page and metadata, and formatting for readability, but it is not yet the definitive version of record. This version will undergo additional copyediting, typesetting and review before it is published in its final form, but we are providing this version to give early visibility of the article. Please note that, during the production process, errors may be discovered which could affect the content, and all legal disclaimers that apply to the journal pertain.

© 2020 Published by Elsevier B.V.

## Highlights

- A new pyrazole and hydrazone derivatives were synthesized.
- The structure of the designed compound was confirmed by spectroscopic methods.
- Anti-proliferative activity and SAR study were evaluated and discussed.
- The carbonic anhydrase (IX & XII) were determined for the most promising compounds.
- Docking study was carried out as well as some physicochemical properties.

Journal Pre-proof

**Novel adamantane-pyrazole and hydrazone hybridized: design, synthesis, cytotoxic evaluation, SAR study and molecular docking simulation as carbonic anhydrase inhibitors**

Mohammed M. S. Wassel<sup>1</sup>, Ahmed Ragab<sup>2,\*</sup>, Gameel A. M. Elhag Ali<sup>2</sup>, Ahmed B. M. Mehany<sup>3</sup>, Yousry A. Ammar<sup>2,\*</sup>

<sup>1</sup>Department of Foot and Mouth Disease, Veterinary Serum and Vaccine Research Institute (VSVRI), Abbasia, Cairo, Egypt

<sup>2</sup>Chemistry Department, Faculty of Science, Al-Azhar University, Nasr City, Cairo 11884, Egypt

<sup>3</sup>Zoology Department, Faculty of Science, Al-Azhar University, Nasr City, Cairo 11884, Egypt

**Abstract**

A series of pyrazole derivatives **4, 5, 6, 12, 13, 14** as well as hydrazone derivatives **7, 10, 11** were synthesized starting from adamantane-1-carbohydrazide as the bioactive core. All newly designed adamantane derivatives were established by **full characterized** using different spectroscopic methods. **The novel derivatives were investigated for their antitumor activity against three cell line MCF-7, HepG-2 and A549. They displayed good IC<sub>50</sub> values ranged between 1.55 to 42.17 μM in comparison to Doxorubicin (IC<sub>50</sub> =3.58-8.19 μM). Surprisingly, adamantane derivatives revealed more sensitivity and selectivity to lung cancer cells (A549) with eight compounds (**4, 5, 9a, 9b, 9c, 12, 13a and 14c**) having IC<sub>50</sub> less than or equal ten micromoles.** The most promising three adamantane derivatives **9a, 12 and 13a** with IC<sub>50</sub> values less than 5 μM were selected to study enzymatic assay for isoenzyme hCAIX and hCAXII. Also, pyrazole core **13a** and **12** showed higher K<sub>I</sub> values than hydrazone derivatives **9a** with submicromolar between (0.085-0.527 μM), in comparison to Acetazolamide (0.041-0.068 μM). **Compound 13a is the most promising derivatives with anti-proliferative (A549) (IC<sub>50</sub>=1.55 ± 0.08 μM) which showed CAIX/XII inhibitory activity (K<sub>I</sub>= 0.085 and 0.14 μM), respectively.** Finally, molecular docking simulation was performed to determine the binding modes and possible interaction of the adamantane derivatives within the active site of 3IAI and 1JD0 for CAIX / XII respectively with low binding affinity.

---

\*Corresponding author: Ahmed Ragab (Ph.D.) Tel.: +202 01009341359; E-mail: [ahmed\\_ragab@azhar.edu.eg](mailto:ahmed_ragab@azhar.edu.eg) & [ahmed\\_ragab7@ymail.com](mailto:ahmed_ragab7@ymail.com).

\*Corresponding authors; Yousry Ahmed Ammar ; E-mail: [yossry@yahoo.com](mailto:yossry@yahoo.com) & [yossry@azhar.edu.eg](mailto:yossry@azhar.edu.eg).

---

**Keywords:** Adamantane; Anti-proliferative activity; Carbonic anhydrase inhibitors; Molecular docking

## 1. Introduction

One of the most significant diseases responsible for worldwide deaths, cancer is a general term used to describe the uncontrolled proliferation of cells resulting from disruptions or dysfunctions of the regulatory signaling pathway [1,2]. Cancer is a complex disease caused by genetic and/or epigenetic changes in one cell or a group of cells [3]. At present, it is the major public concerned hotspot across the globe [4]. Deaths owing to cancer are predicted to continue increasing by 3 million deaths in 2030 [5]. Lung, breast, colon, and melanoma cancers are the most recorded types in developing and underdeveloped countries [6]. The emergence and growing resistance to the currently obtainable chemotherapeutic agents demonstrates a critical need for producing novel, more powerful, and selective anticancer drugs [7]. Lung cancer is one of the most frequently diagnosed malignancies in addition to that leads to cancer-associated mortality [8–10]. Due to the histopathological results, lung cancer is categorized into two main subgroups: small cell lung carcinoma (SCLC) and non-SCLC (NSCLC). NSCLCs include 85% of all lung cancer cases, that are classified into three types as adenocarcinoma, squamous cell carcinoma, and large cell carcinoma [11]. Carbonic anhydrases (CAs) enzymes which undergo a physiological reaction that hydrates  $\text{CO}_2$  reversibly into a proton and  $\text{HCO}_3^-$  [12–15]. The human carbonic anhydrase (hCA) consists of fifteen different isoforms; it differs in sequences, mainly for expression tissue, localization, and catalytic activity [16,17]. There are different physiological processes containing electrolyte secretion in a variety of tissues and organs, transport of  $\text{CO}_2$  / bicarbonate metabolizing tissues and lungs, pH and  $\text{CO}_2$  homeostasis, respiration, bone resorption, biosynthetic reactions and tumorigenicity, calcification, and many other Pathophysiological processes [18]. Nowadays, the current approaches to the treatment of cancer, including surgery, radiotherapy, and chemotherapy either alone or in combination, but due to metastasis (spreading of the disease to other parts of the body), only 40 percent of patients can be cured and are associated with a high mortality rate [19]. Chemotherapy is the main weapon against neoplastic diseases, and most of the anticancer drugs clinics are of synthetic origin [20]. These chemopreventive drugs act by various mechanisms that may involve inhibition of

initiation, promotion, **progression, and cancerous cells metastasis**. However, during this process, a normal cell can be exposed to toxic [21].

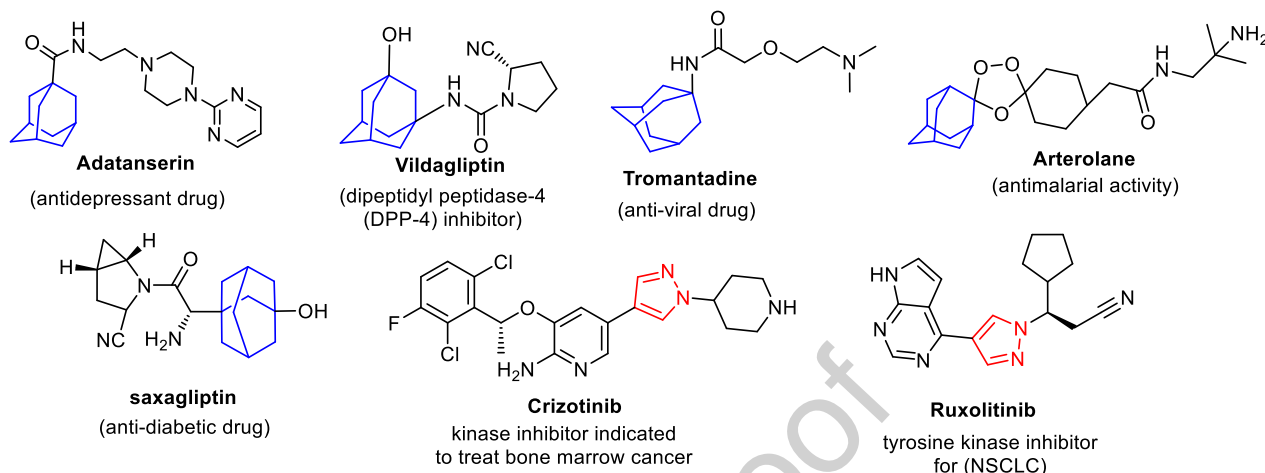


**Figure 1:** Drugs containing Adamantane nucleus or pyrazole moiety.

Many anticancer drugs have been approved, but most of them non-specific and have many side effects during chemotherapy [22,23], so new medicines that are effective in drug-resistant cancers need to be developed [24]. Moreover, there is an urgent **need to design** and synthesize new drugs that have potency and highly selective to cancer cells with least or no toxicity to healthy cells. Adamantane derivatives have been found to interfere with various enzymes and possess a variety of therapeutic activities [25], such as anti-inflammatory [24,26,27], anti-viral as Tromantadine [28–31] and anti-anticancer activities [32,33]. Adamantyl moiety hybrid with several molecules to enhance the biological availability of the designed compounds, and an example of that is **Adapalene** that used as acne vulgaris therapy that containing adamantane in the main skeleton as well as naphthalene derivatives that relatively high lipophilicity [34] (**Fig. 1**). Adamantane nucleus present in many drugs as Vildagliptin (dipeptidyl peptidase-4 (DPP-4) inhibitor) [35], Adatanserin (anti-depressant) [36], and Saxagliptin (hypoglycemic drug) [37], Arterolane (antimalarial activity) [38] (**Fig. 1**). Furthermore, pyrazoles are an important class of heterocyclic compounds that promising scaffolds in medicinal chemistry [39–42]. Crizotinib and Ruxolitinib are examples of pyrazole-containing drugs used for treating myeloproliferative neoplasm and non-small cell lung carcinoma (NSCLC), respectively [43] (**Fig. 1**). Also, **hydrazones are an essential class** of compounds due to their flexibility and structural similarities with various natural

substances of biological importance [44,45]. **Hydrazone derivatives** have an imine (N=C) group, **that** plays a significant role in the mechanism of transformation and racemization reaction in the biological system [46–48]. Because of these facts and in continuation of our efforts in designing new bioactive compounds [49–52]. We have designed and synthesized a novel pyrazole and hydrazine derivatives bearing adamantane bioactive core as a promising heterocyclic scaffold and screened for anticancer activity and tested the most promising to carbonic anhydrase and therefore the molecular docking simulation and some drug-likeness parameter were evaluated to find potential candidates.

## 2. Experimental

### 2.1. Chemistry

Uncorrected melting points are recorded on digital Gallen Kamp MFB-595 instrument. The IR spectra (KBr) ( $\text{cm}^{-1}$ ) were measured on a Shimadzu 440 spectrophotometer.  $^1\text{H}$  NMR spectra ( $\delta$ , ppm) were obtained in deuterated dimethyl sulfoxide (DMSO-*d*<sub>6</sub>) or deuterated chloroform ( $\text{CDCl}_3$ ) and  $^{13}\text{C}$  NMR at 100 MHz, spectra were obtained on a Bruker spectrometer (400 MHz) spectrometer, using TMS as an internal standard; chemical shifts are reported as  $\delta$  ppm units. The data were presented as follows: chemical shift, multiplicity (**s= singlet**, **d= doublet**, **t= triplet**, q= quartet, m= multiplet, br= broad, app= apparent), coupling constant(s) in Hertz (Hz), and integration. Mass spectra were recorded on Thermo Scientific ISQLT mass spectrometer at the Regional Center for Mycology and Biotechnology, Al-Azhar University. Elemental analyses were carried **out in Microanalytical** Unit, Cairo University, Cairo, Egypt. Anticancer activity was carried out in local strain **identified in the Regional** Center for genetic engineering, faculty of **Science (Boys)**, Al-Azhar University, and **Carbonic Anhydrase** IX and XII were carried out in (VACSERA), Cairo, Egypt.

#### 1-(Adamantane-1-carbonyl)-5-amino-3-(methylthio)-1H-pyrazole-4-carbonitrile (4)

A mixture of adamantane-1-carbohydrazide (**3**) (0.01mol), 2-(*bis*(methylthio)methylene)malononitrile (0.01mol), in absolute ethanol (20 mL) catalyzed with piperidine (0.5 mL) was heated under reflux for 2h. The solid product formed was collected by filtration and crystallized from ethanol.

Orange powder, yield 72 %, M.p.= 238-240 °C, IR (KBr,  $\text{cm}^{-1}$ ): 3231, 3166 ( $\text{NH}_2$ ), 2911, 2849 (CH aliph.) 2215, (CN) and 1693 (C=O);  $^1\text{H}$  NMR (400 MHz, DMSO)  $\delta$  1.63-1.70 (m, 6H, 3 $\text{CH}_2$ ), 2.02 (s, 3H, 3CH), 2.18 (s, 6H, 3 $\text{CH}_2$ ), 2.55 (s, 3H, S-Me), 8.11 (s, 2H,  $\text{NH}_2$ , exchangeable by  $\text{D}_2\text{O}$ );  $^{13}\text{C}$  NMR (101 MHz, DMSO)  $\delta$  9.11 (S-Me), 27.70, 27.92, 28.03, 36.30, 36.57, 37.57, 38.97, 44.54, 46.21 (Adamant. Cs), 71.47 (C-CN), 113.42 (CN), 152.00 (C=N), 157.08 (C- $\text{NH}_2$ ), 178.40 (C=O); MS (EI, 70 eV):  $m/z$  (%) = 316.67 [ $\text{M}^+$ ] (26.94%), 153 (100%); Anal. Calcd for  $\text{C}_{16}\text{H}_{20}\text{N}_4\text{OS}$  (316.42): C; 60.73, H; 6.37; N; 17.71. Found: C; 60.43, H; 6.32, N; 18.04.

### 1-(Adamantane-1-carbonyl)-5-amino-1H-pyrazole-4-carbonitrile (5)

To a solution of adamantane-1-carbohydrazide (**3**) (0.01 mol) in absolute ethanol (20 mL) containing a catalytic amount of piperidine (0.5 mL) ethoxy methylene malononitrile (0.01 mol) was added. The reaction mixture was heated under reflux for 3h. The solid product formed was collected by filtration and recrystallized from ethanol.

White crystals, yield 69 %, M.p.= 170-172 °C. IR (KBr,  $\text{cm}^{-1}$ ): 3416, 3229 ( $\text{NH}_2$ ), 2906 (CH aliph.) 2222 (CN), and 1702 (C=O);  $^1\text{H}$  NMR (400 MHz, DMSO)  $\delta$  1.71 (s, 6H, 3 $\text{CH}_2$ ), 2.03 (s, 3H, 3CH), 2.18 (s, 6H, 3 $\text{CH}_2$ ), 7.89 (s, 1H, pyrazole-H), 7.98 (s, 2H,  $\text{NH}_2$ , exchangeable with  $\text{D}_2\text{O}$ );  $^{13}\text{C}$  NMR (101 MHz, DMSO)  $\delta$  27.90, 36.43, 37.70, 44.75 (Adamant. Cs), 72.15 (C-CN), 114.32 (CN), 143.44 (C=N), 156.24 (C- $\text{NH}_2$ ), 179.34 (C=O); MS (EI, 70 eV):  $m/z$  (%) = 270.47 [ $\text{M}^+$ ] (10.34%), 115 (100%); Anal. Calcd for  $\text{C}_{15}\text{H}_{18}\text{N}_4\text{O}$  (270.34): C; 66.64, H; 6.71; N; 20.73. Found: C; 66.98, H; 6.43, N; 20.51.

### N-(1-(Adamantane-1-carbonyl)-4-cyano-1H-pyrazol-5-yl)acetamide (6)

To a solution of 5-amino-1H-pyrazole derivative **5** (0.01 mol) acetic anhydride (10 mL) was added. The reaction mixture was heated under reflux for 1h. The solid product formed after cooling was collected by filtration and crystallized from methanol.

Yellow powder, yield 69 %, M.p. = 110-112 °C. IR (KBr,  $\text{cm}^{-1}$ ): 3258 (NH), 2910 (CH. aliph.) 2230, (CN), and 1694 (br. C=O);  $^1\text{H}$  NMR (400 MHz, DMSO)  $\delta$  1.66 (s, 3H,  $\text{CH}_3$ ), 1.79 (s, 6H, 3 $\text{CH}_2$ ), 1.96 (s, 3H, 3CH), 2.06 (s, 6H, 3 $\text{CH}_2$ ), 8.27 (s, 1H, pyrazole-H), 10.69 (s, 1H, NH, exchangeable with  $\text{D}_2\text{O}$ );  $^{13}\text{C}$  NMR (101 MHz, DMSO)  $\delta$  23.07 ( $\text{CH}_3$ ), 27.85, 36.50, 38.96, 38.96 (Adamant. Cs), 75.27 (C-CN), 114.17 (CN), 160.17 (C=N), 162.39 (C-NH), 168.78, 178.98

(C=O); MS (EI, 70 eV):  $m/z$  (%) = 312.72 [ $M^+$ ] (55.22%), 94 (100%); Anal. Calcd. for  $C_{17}H_{20}N_4O_2$  (312.37): C; 65.37, H; 6.45; N; 17.94. Found: C; 65.12, H; 6.74, N; 18.12.

### Ethyl-3-(2-(adamantane-1-carbonyl)hydrazinyl)-2-cyanoacrylate (7)

A mixture of adamantane-1-carbohydrazide (**3**) in (20 mL) ethanol catalyzed with piperidine (0.5 mL) ethoxy methylene ethyl cyanoacetate (0.01 mol) was added. The reaction mixture was heated under reflux for 3h. The solid product formed was collected by filtration and crystallized from ethanol.

Yellow powder, yield 72 %, M.p.= 198-200 °C; IR (KBr,  $cm^{-1}$ ): 3246 (NH), 2907 (CH aliph.) 2213, (CN) and 1710,1671 (C=O);  $^1H$  NMR (400 MHz,  $CDCl_3$ )  $\delta$  1.32 (t,  $J = 6.7$  Hz, 3H,  $\underline{CH_3}$ - $CH_2$ -), 1.74-1.77 (m, 6H, 3 $CH_2$ ), 1.91 (s, 5H, 3CH+ $CH_2$ ), 2.09 (s, 4H, 2 $CH_2$ ), 2.28 (s, 1H, vinylic- $H$ ), 4.26 (q,  $J = 6.7$  Hz, 2H,  $CH_3$ - $\underline{CH_2}$ -), 7.31, 8.09 (2s, 2H, 2NH, exchangeable with  $D_2O$ ); MS (EI, 70 eV):  $m/z$  (%) = 317.55 [ $M^+$ ] (25.51%), 190 (100%); Anal. Calcd for  $C_{17}H_{23}N_3O_3$  (317.39): C, 64.33; H, 7.30; N, 13.24; Found: C, 64.67; H, 7.13, N, 13.07.

### Synthesis of hydrazone derivatives 9a-c

To a solution of adamantane-1-carbohydrazide (**3**) in (20 mL) ethanol catalyzed with acetic acid (0.5 mL) 1,3-dicarbonyl derivatives (3-methylpentane-2,4-dione, benzoylacetone and ethyl acetoacetate) (0.01 mol) was added. The reaction mixture was heated under reflux for 4-7h. The solid product formed was collected by filtration and recrystallized from ethanol.

### *N'*-(3-Methyl-4-oxopentan-2-ylidene)adamantane-1-carbohydrazide (9a)

White crystals, yield 73%, M.p.= 83-85 °C; IR (KBr,  $cm^{-1}$ ): 3271 (NH), 2891, 2961, 2900, 2850 (CH aliph.) and 1732, 1658 (C=O);  $^1H$  NMR (400 MHz,  $CDCl_3$ )  $\delta$  1.24 – 1.27 (m, 3H,  $CH_3$ ), 1.36–1.40 (m, 3H,  $CH_3$ ), 1.71-1.74 (m, 6H, 3 $CH_2$ ), 1.87 (s, 3H,  $CH_3$ ), 1.95 (s, 5H, 3CH+ $CH_2$ ), 2.07 (s, 4H, 2 $CH_2$ ), 4.13-4.19 (m, 1H, -CH-), 8.36 (s, 1H, NH exchangeable with  $D_2O$ );  $^{13}C$  NMR (101 MHz,  $CDCl_3$ )  $\delta$  14.17( $CH_3$ ), 21.82 ( $CH_3$ ), 27.83, 27.89, 27.98, 28.44, 36.34, 36.40, 36.44, 38.67, 38.83, 39.09, 40.76, 48.49 (Adamant. Cs +  $CH_3$ ), 154.57 (C=N), 172.77, 203.81 (2C=O); MS (EI, 70 eV):  $m/z$  (%) = 290.73 [ $M^+$ ] (21.41%), 227.45 (100%); Anal. Calcd for  $C_{17}H_{26}N_2O_2$  (290.41): C, 70.31; H, 9.02; N, 9.65; Found: C, 70.51; H, 9.14; N, 9.47.

***N'*-(3-Oxo-1-phenylbutylidene)adamantane-1-carbohydrazide (9b)**

Colorless crystals, yield 73%, M.p.= 218-220 °C; IR (KBr, cm<sup>-1</sup>): 3294 (NH), 3062, 3020 (CH Aro.), 2904, 2854 (CH aliph.) and 1693 (C=O); <sup>1</sup>H NMR (400 MHz, CDCl<sub>3</sub>) δ 1.73 (s, 6H, 3CH<sub>2</sub>), 1.90 (s, 3H, CH<sub>3</sub>), 2.02 (s, 5H, 3CH+CH<sub>2</sub>), 2.11 (s, 4H, 2CH<sub>2</sub>), 2.74-2.79 (d, *J*= 18.4 Hz, 1H), 3.11-3.16 (d, *J*= 18.8 Hz, 1H), 7.31 (d, 3H, Ar-H), 7.32 (s, 1H, Ar-H), 7.33 (s, 1H, Ar-H), 7.86 (s, 1H, NH exchangeable with D<sub>2</sub>O), <sup>13</sup>C NMR (101 MHz, CDCl<sub>3</sub>) δ 27.90, 28.28, 28.43, 36.34, 36.71, 37.41, 38.77, 38.93, 42.28 (Adamant. Cs), 52.52 (CH<sub>2</sub>), 123.53, 126.27, 126.99, 127.72, 128.22, 128.63 (Ar-Cs), 152.46 (C=N), 176.77, 193.83 (2C=O); MS (EI, 70 eV): *m/z* (%) = 338 [M<sup>+</sup>] (38.86 %), 134.24 (100%); Anal. Calcd for C<sub>21</sub>H<sub>26</sub>N<sub>2</sub>O<sub>2</sub> (338.45): C, 74.53; H, 7.74; N, 8.28; Found: C, 74.64; H, 7.58; N, 8.39.

**Ethyl-3-(2-(adamantane-1-carbonyl)hydrazono)butanoate (9c)**

White powder, yield 73%, M.p = 92-94°C. IR (KBr, cm<sup>-1</sup>): 3236 (NH), 2908, 2850 (CH. aliph.) and 1678, 1728 (C=O); <sup>1</sup>H NMR (400 MHz, CDCl<sub>3</sub>) δ 1.25 (t, *J* = 7.0 Hz, 3H, CH<sub>3</sub>-CH<sub>2</sub>-), 1.72 (s, 6H, 3CH<sub>2</sub>), 1.90 (s, 3H, CH<sub>3</sub>), 1.91 (s, 5H, 3CH+CH<sub>2</sub>), 2.06 (s, 4H, 2CH<sub>2</sub>), 2.33 (s, 2H, CH<sub>2</sub>), 3.70 (q, *J* = 7.0 Hz, 2H, CH<sub>3</sub>-CH<sub>2</sub>-), 8.62 (s, 1H, NH exchangeable with D<sub>2</sub>O); <sup>13</sup>C NMR (101 MHz, CDCl<sub>3</sub>) δ 14.12 (CH<sub>3</sub>-CH<sub>2</sub>-), 27.66, 27.83, 27.98, 28.05, 36.34, 36.46, 38.66, 39.09, 40.05 (Adamant. Cs), 58.45(CH<sub>2</sub>), 61.53, (CH<sub>3</sub>-CH<sub>2</sub>-), 147.17 (C=N), 165.03, 173.47(C=O); MS (EI, 70 eV): *m/z* (%) = 306.74 [M<sup>+</sup>] (19.00%), 288.23 (100%); Anal. Calcd for C<sub>17</sub>H<sub>26</sub>N<sub>2</sub>O<sub>3</sub> (306.41): C, 66.64; H, 8.55; N, 9.14; Found C, 66.35; H, 8.64; N, 9.02.

**Synthesis of *N'*-((2-chloroquinolin-3-yl)methylene)adamantane-1-carbohydrazide (11)**

A mixture of adamantane-1-carbohydrazide **3** (0.01mol), and 2-chloro-3-formyl-quinoline in absolute ethanol (20 mL) catalyzed with acetic acid (0.5 mL), then the reaction heated under reflux condition. The solid product formed when cooled then washed several time with ethanol then collected by filtration and finally crystalized from a mixture of ethanol and with a few drops' methanol.

Yellow powder, yield 65.7%, M.p.= 250-252 °C. IR (KBr, cm<sup>-1</sup>): 3261 (NH), 2908 (CH. aliph.) and 1663 (C=O), <sup>1</sup>H NMR (400 MHz, CDCl<sub>3</sub>) δ 1.73 (s, 6H, 3CH<sub>2</sub>), 1.79 (s, 3H, 3CH), 2.12 (s, 6H, 3CH<sub>2</sub>), 6.02 (s, 1H, NH; exchangeable with D<sub>2</sub>O), 7.37 (t, *J* = 7.5 Hz, 1H, Ar-H), 7.66 (t, *J* =

7.7 Hz, 1H, Ar-H), 7.77 (d,  $J = 8.0$  Hz, 1H, Ar-H), 7.83 (d,  $J = 8.4$  Hz, 1H, Ar-H), 8.45 (s, 1H, CH-methylinic), 8.66 (s, 1H, Quinoline-*H4*); Anal. Calcd for  $C_{21}H_{22}ClN_3O$  (367.88): C, 68.56; H, 6.03; N, 11.42; Found: C, 68.71; H, 5.96; N, 11.22.

### Synthesis of *N'*-((5-phenyl-4-(*p*-tolyl)-1*H*-pyrazol-3-yl)methylene)adamantane-1-carbohydrazide (12)

To a solution of adamantane-1-carbohydrazide **3** (0.01 mol) in ethanol (10 mL), 5-phenyl-4-(*p*-tolyl)-1*H*-pyrazole-3-carbaldehyde was added. The reaction mixture was heated under reflux for **3 h**, and the solution was allowed to **be cooled, then** the products were collected by filtration and recrystallized from ethanol.

White powder, yield 68%, M.p.= 210-212°C; IR (KBr,  $cm^{-1}$ ): 3240 (NH), 2904, 2850 (CH. aliph.) and 1647 (C=O);  $^1H$  NMR (400 MHz,  $CDCl_3$ )  $\delta$  1.73 (d, 6H, 3CH<sub>2</sub>), 1.95 (s, 6H, 3CH<sub>2</sub>), 2.07 (s, 3H, 3CH-), 2.41 (s, 3H, CH<sub>3</sub>), 7.26 (s, 1H, Ar-H), 7.28 (s, 1H, Ar-H), 7.31 (d,  $J = 7.4$  Hz, 1H, Ar-H), 7.45 (t,  $J = 7.9$  Hz, 2H, Ar-H), 7.51 (d,  $J = 8.0$  Hz, 2H, Ar-H), 7.75 (d,  $J = 7.7$  Hz, 2H, Ar-H), 8.18 (s, 1H, CH methine), 8.60, 8.93 (s, 2H, 2NH; exchangeable with D<sub>2</sub>O);  $^{13}C$  NMR (101 MHz,  $CDCl_3$ )  $\delta$  21.34 (CH<sub>3</sub>), 27.99, 36.39, 39.02, 40.39 (Adamant. Cs), 116.19, 119.16, 126.69, 127.02, 128.56, 129.35, 129.41, 129.50, 138.46 (Ar-Cs), 139.43, 140.96 (C=C), 153.06 (C=N), 173.91 (C=O); MS (EI, 70 eV):  $m/z$  (%) = 438.34 [ $M^+$ ] (21.77%), 199.84 (100%); Anal. Calcd for  $C_{28}H_{30}N_4O$  (438.58): C, 76.68; H, 6.90; N, 12.78; Found: C, 76.62; H, 6.96; N, 12.65.

### Synthesis of (adamantan-1-yl)(3,5-diamino-4-(aryldiazenyl)-1*H*-pyrazol-1-yl)methanone (13a,b)

To a solution of adamantane-1-carbohydrazide **3** (0.01 mol), in absolute ethanol (20 mL), arylhydrazonyl malononitrile derivatives (0.01 mol) **were added**. The reaction mixture was heated under reflux for **2-5h**. The solid product formed was collected by filtration and recrystallized from ethanol to give **(13a, b)**.

#### (Adamantan-1-yl)(3,5-diamino-4-(phenyldiazenyl)-1*H*-pyrazol-1-yl)methanone (13a)

Yellow powder, yield 71.2 %, m.p.= 270-272°C; IR (KBr,  $cm^{-1}$ ): 3543, 3480, 3332, 3281 (NH<sub>2</sub>), 3072 (CH arom.), 2908, 2895, 2849 (CH. aliph.) and 1663 (C=O);  $^1H$  NMR (400 MHz, DMSO) 1.77 (s, 6H, 3CH<sub>2</sub>), 1.95 (s, 3H, 3CH-), 2.03 (s, 6H, 3CH<sub>2</sub>), 6.13 (s, 2H, NH<sub>2</sub>, exchangeable with

D<sub>2</sub>O), 7.27-7.30 (m, 1H, Ar-H), 7.42 (t, 1H,  $J = 7.2$  Hz, Ar-H), 7.66 (t, 1H,  $J = 7.2$  Hz, Ar-H), 7.78 (d, 1H,  $J = 7.4$  Hz, Ar-H), 8.00 (d, 1H,  $J = 7.2$  Hz, Ar-H), 8.82 (s, 2H, NH<sub>2</sub>, exchangeable with D<sub>2</sub>O); <sup>13</sup>C NMR (101 MHz, DMSO)  $\delta$  27.85, 28.01, 28.03, 28.17, 36.56, 36.59, 37.40, 44.08 (Adamant. Cs), 112.98, 119.37, 121.48, 124.40, 128.41, 128.40, 129.11, 129.35 (Ar-Cs+ pyrazole C), 153.45 (2C-NH<sub>2</sub>), 176.78(C=O); MS (EI, 70 eV):  $m/z$  (%) = 364.54 [ $M^+$ ] (23.49%), 306.15 (100%), Anal. Calcd for C<sub>20</sub>H<sub>24</sub>N<sub>6</sub>O (364.45): C, 65.91; H, 6.64; N, 23.06, Found: C, 65.87; H, 6.58; N, 23.21.

**(Adamantan-1-yl)(3,5-diamino-4-((*p*-methoxyphenyl)diazenyl)-1*H*-pyrazol-1-yl)methanone (13b)**

Red powder, yield 75%, m.p.= 280-282 °C; IR (KBr, cm<sup>-1</sup>): 3462, 3442, 3378, 3348 (NH<sub>2</sub>), 3062 (CH arom.), 2903, 2849 (CH. aliph.) and 1666 (C=O); <sup>1</sup>H NMR (400 MHz, DMSO) 1.73-1.76 (m, 6H, 3CH<sub>2</sub>), 2.02 (s, 3H, 3CH-), 2.24 (s, 6H, 3CH<sub>2</sub>), 3.81 (s, 3H, OCH<sub>3</sub>), 6.07 (s, 2H, NH<sub>2</sub>, exchangeable with D<sub>2</sub>O), 6.98 (d, 2H, Ar-H), 7.76 (d, 2H, Ar-H), 8.09 (s, 2H, NH<sub>2</sub>, exchangeable with D<sub>2</sub>O); <sup>13</sup>C NMR (101 MHz, DMSO)  $\delta$  28.05, 36.37, 37.45, 39.06, 39.37 (Adamant. Cs), 55.85 (OCH<sub>3</sub>), 112.30, 114.57, 122.41, 147.64 (2C-NH<sub>2</sub>), 159.86 (C-OCH<sub>3</sub>), 178.77 (C=O); MS (EI, 70 eV):  $m/z$  (%) = 394.49 [ $M^+$ ] (24.70%), 93.40 (100%); Anal. Calcd for C<sub>21</sub>H<sub>26</sub>N<sub>6</sub>O<sub>2</sub> (394.48): C, 63.94; H, 6.64; N, 21.30, Found: C, 64.07; H, 6.52; N, 21.45.

**Synthesis of 1-((adamantan-1-yl)methyl)-4,5-dihydro-1*H*-pyrazole derivatives 14a-c**

A mixture of adamantane-1-carbohydrazide **3** (0.01 mol), in absolute ethanol (20 mL) and chalcone derivatives (0.01 mol) were heated under reflux for 4-6h. The solid product formed was collected by filtration and recrystallized from ethanol to give (14a-c).

**(Adamantan-1-yl)(5-(*p*-methoxyphenyl)-3-phenyl-1*H*-pyrazol-1-yl)methanone (14a)**

Faint yellow powder, yield 64%, M.p.= 102-104 °C; IR (KBr, cm<sup>-1</sup>): 3069, 3032 (CH arom.), 2969, 2908, 2843 (CH aliph.) and 1655 (C=O); <sup>1</sup>H NMR (400 MHz, DMSO)  $\delta$  1.64-1.66 (m, 6H, 3CH<sub>2</sub>), 1.76 (s, 3H, 3CH), 1.94 (s, 6H, 3CH<sub>2</sub>), 3.83 (s, 3H, OCH<sub>3</sub>), 7.03 (d,  $J = 8.7$  Hz, 2H, Ar-H), 7.57 (t,  $J = 7.5$  Hz, 2H, Ar-H), 7.67 (t,  $J = 7.3$  Hz, 1H, Ar-H), 7.87 (d,  $J = 8.7$  Hz, 2H, Ar-H), 8.14 (d,  $J = 7.2$  Hz, 2H, Ar-H), 8.69 (s, 1H, CH-pyrazole); <sup>13</sup>C NMR (101 MHz, DMSO)  $\delta$  27.96, 28.04, 36.61 (Adamant. Cs), 54.90 (OCH<sub>3</sub>), 123.26, 128.92, 129.18, 129.32, 129.39, 129.68, 129.83, 130.30, 131.01, 134.17, 135.39 (Ar-Cs), 142.61, 144.18 (C=C), 176.77 (C-OCH<sub>3</sub>), 188.95

(C=O); Anal. Calcd for C<sub>27</sub>H<sub>28</sub>N<sub>2</sub>O<sub>2</sub> (412.53): C; 78.61, H; 6.84, N; 6.79, Found: C; 78.23, H; 6.27, N; 7.01.

**(Adamantan-1-yl)(3,5-di-*p*-tolyl-1*H*-pyrazol-1-yl)methanone (14b)**

Yellow powder, yield 72 %, M.p.= 108-110 °C. IR (KBr, cm<sup>-1</sup>): 3032 (CH arom.), 2290, 2851 (CH. aliph.) and 1655 (C=O); <sup>1</sup>H NMR (400 MHz, DMSO) δ 1.64 (d, *J* = 7.3 Hz, 6H, 3CH<sub>2</sub>), 1.76 (s, 6H, 3CH<sub>2</sub>), 1.94 (s, 3H, 3CH), 2.37 and 2.41 (2s, 6H, 2CH<sub>3</sub>), 7.27-7.33 (m, 1H, Ar-H), 7.39 (d, *J* = 8.0 Hz, 2H, Ar-H), 7.53 (d, *J* = 8.4 Hz, 1H, Ar-H), 7.65 – 7.75 (m, 1H, Ar-H), 7.94 (d, *J* = 8.4 Hz, 2H, Ar-H), 8.08 (d, *J* = 8.0 Hz, 1H, Ar-H), 8.69 (s, 1H, CH-pyrazole); MS (EI, 70 eV): *m/z* (%) = 410.67 [M<sup>+</sup>] (22.26%), 392.45 (100%); Anal. Calcd for C<sub>28</sub>H<sub>30</sub>N<sub>2</sub>O (410.56): C, 81.91; H, 7.37; N, 6.82, Found: C, 81.71; H, 7.48; N, 6.75.

**(Adamantan-1-yl)(5-(*p*-chlorophenyl)-3-phenyl-1*H*-pyrazol-1-yl)methanone (14c)**

Yellow powder, yield 69.4 %, M.p.=118-120°C; IR (KBr, cm<sup>-1</sup>): 3056 (CH arom.), 2989, 2850 (CH.aliph.) and 1657 (C=O); <sup>1</sup>H NMR (400 MHz, DMSO) δ 1.64 (s, 6H, 3CH<sub>2</sub>), 1.77 (s, 6H, 3CH<sub>2</sub>), 1.93 (s, 3H, 3CH), 7.02 (d, *J* = 8.4 Hz, 2H, Ar-H), 7.36 (d, *J* = 8.0 Hz, 2H, Ar-H), 7.73-7.77 (m, 1H, Ar-H), 7.84 (d, *J* = 8.8 Hz, 2H, Ar-H), 8.06 (d, *J* = 8.0 Hz, 2H, Ar-H), 8.70 (s, 1H, , CH-pyrazole); <sup>13</sup>C NMR (101 MHz, DMSO) δ 25.77, 28.05, 36.60 (Adamant. Cs), 114.84, 119.98, 127.82, 128.99, 129.74, 131.17, 135.78, 143.73, 144.08 (C=C), 176.79 (C=N), 188.91(C=O); MS (EI, 70 eV): *m/z* (%) = 416.10 [M<sup>+</sup>] (16.89%), 293.63 (100%), Anal. Calcd for C<sub>26</sub>H<sub>25</sub>ClN<sub>2</sub>O (416.95): C, 74.90; H, 6.04; N, 6.72, Found: C, 74.75; H, 5.84; N, 6.57.

## 2.2. Biological evaluation

### 2.2.1. Anti-proliferative activity

*In vitro* cytotoxicity of all the newly designed and synthesized adamantane nucleus were tested against three human tumours cell lines including human breast adenocarcinoma cell line (MCF-7), human hepatocellular carcinoma cell line (HepG-2) as well as human lung adenocarcinoma epithelial cells (A549), they were obtained from VACSERA- Cell Culture Unit, Cairo, Egypt, by using colorimetric assay method (SRB) under standard conditions according to our reported methods [45, 52].

### 2.2.2. Carbonic anhydrase assay

Carbonic anhydrase (CA) IX and XII inhibition activities were evaluated using Recombinant Human Carbonic Anhydrase IX / XII Protein, CF Kit, that obtained from R&D Systems (Minneapolis, MN, USA), following the same instructions from the manufacturer protocol that measured by its esterase activity according to reported methods [53]. The Assay procedure involved material as (1) Assay Buffer: 12.5 mM Tris, 75 mM NaCl, pH 7.5, (2) Recombinant Human Carbonic Anhydrase IX/CA9 (rhCA9) (Catalog # 2188-CA) or Carbonic Anhydrase XII/CA12 (rhCA12) (Catalog # 2190-CA), (3) Substrate: 4-Nitrophenyl Acetate (4-NPA) (Sigma, Catalog # N8130), 100 mM stock in acetone. The following steps involving the producer as; firstly, both rhCAIX or rhCAXII was diluted to 20 ng/ $\mu$ L and substrate (4-Nitrophenyl acetate) also diluted to 2 mM by using a buffer. In 96-well Clear Plate (Costar, Catalog # 92592), load 50  $\mu$ L of 20 ng/ $\mu$ L rhCA12, and start the reaction by adding 50  $\mu$ L of 2 mM Substrate to wells. Include a substrate blank containing 50  $\mu$ L assay Buffer and 50  $\mu$ L of 2 mM 4-Nitrophenyl acetate. Inhibitory effect of the three compounds were compared with Acetazolamide were obtained by different inhibitor concentrations where the tested compound and standard dissolved in DMSO (0.1 mM) with dilution from (10 nM) up to (0.01 nM) by using distilled water and all compounds were tested in triplicate at each concentration used to form the enzyme-inhibitor complex. Read absorbance at a wavelength of 400 nm (bottom read) in kinetic mode for 5 minutes. The calculations were performed as per the kit guidelines, where a specific activity calculated by the following equation:

$$\text{Specific Activity (pmol/min/}\mu\text{g)} = \frac{\text{Adjusted Vmax* (OD/min)} \times \text{Conversion Factor** (pmol/OD)}}{\text{amount of enzyme (}\mu\text{g)}}$$

Control cuvette activity was acknowledged as 100% in the absence of inhibitor, and an activity % – [inhibitor] graph was drawn for each inhibitor then the inhibitory efficacy was calculated by using classic Michaels Menten kinetics according to reported method [54].

### 2.2.3. Molecular docking

Study of molecular docking of the adamantane derivatives and the standard drug was performed according to the described reported method under standard protocol and methods [55], using Molecular Operating Environment (MOE) software version 2008.10. The X-ray crystallography

structure of both CA IX (PDB: 3IAI) and CA XII (PDB: 1JD0) with original ligand 5-acetamido-1,3,4-thiadiazole-2-sulfonamide (AZM) inhibitor [56] downloaded from protein data bank [57]. Protein was prepared by protonated 3D and removed the water molecule and ligand that not implicated in the active site. The active site then generated with the default protocol. Trigonal matcher was selected as placement method and London dG as docking score energy using  $Zn^{+2}$  ion chelate as a constrain for molecular docking. Docking process was firstly performed by self-docking of original ligand AZM in the active site, and the evaluation of the RMSD values for CA IX (PDB: 3IAI) and CA XII (PDB: 1JD0) were 1.02 and 1.06 Å respectively. (binding of co-crystallized ligand and docking score energy with the figure in supplementary material file). The newly designed compounds were generated from Chemdraw14.0 then subjected to protonate 3D and minimize energy and finally washed the structure and saved as mdb file as ligand atom that then used in docking protocol after replaced the co-crystalized AZM and under the same methods.

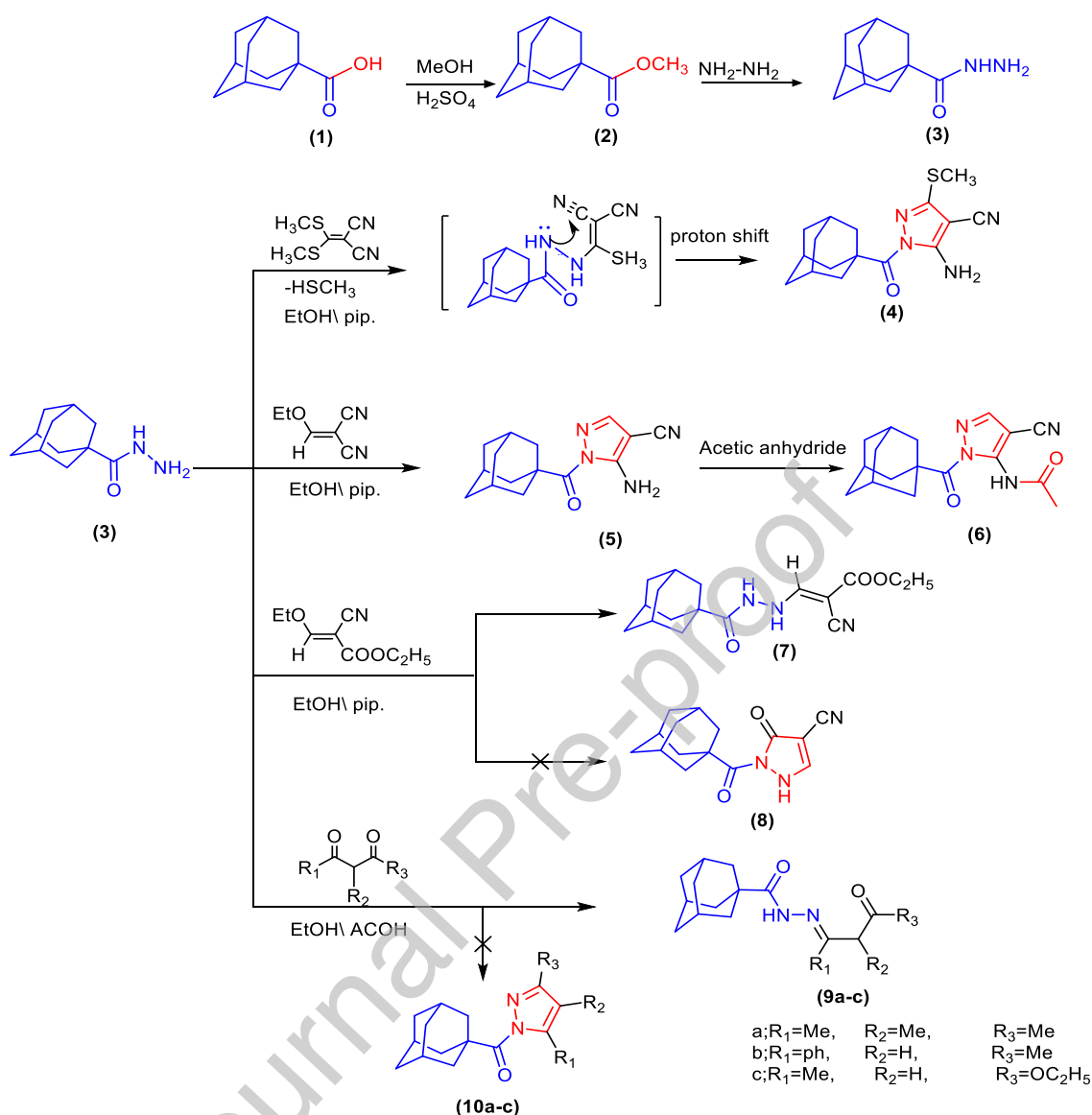
### 3. Results and discussion

#### 3.1. Chemistry

The synthetic strategy to achieve the target compounds pyrazole or hydrazone containing adamantane derivatives 4-14 are shown in schemes 1 & 2. Adamantan-1-carbohyrazide (3) that used as key starting material prepared according to the reported method [58]. The reaction of adamantane-1-carbohyrazide 3 with bis(thiomethyl)methylene malononitrile and ethoxy methylene malononitrile to afforded 2-amino pyrazole derivatives 4 and 5. The reaction proceeds via an addition-elimination mechanism where the amino group of hydrazide derivatives act as nucleophilic that attack the  $\beta$ -carbon of ethylene dinitrile derivatives followed by elimination of methanethiol ( $CH_3SH$ ), followed by cyclization (that involve addition and as well as proton shift) to afford the pyrazole enamionitriles derivatives 4, 5.

IR spectrum of compound 4 showed absorption bands at 3404, 3304, 3231, 3166, for two amino groups besides, 2911, 2849, 2215 and 1693  $cm^{-1}$  corresponding to adamantane CH, CN, and carbonyl group respectively. Its  $^1H$  NMR spectrum of compound 4 showed a significant three peaks at  $\delta$  1.63-1.70, 2.02 and 2.18 ppm related to protons of adamantyl that appear as multiplet and two singlet signals. Furthermore, two-singlet signals were appearing at  $\delta$  2.55 and 8.11 ppm

for thiomethyl and the amino groups, respectively, and the amino group was exchangeable by D<sub>2</sub>O. <sup>13</sup>C NMR spectrum of **compound 5** displayed signals for adamantyl carbons between  $\delta$  27.9-44.75 ppm besides, five signals at  $\delta$  72.15, 114.32, 143.44, 156.24, 179.34 for the carbon of pyrazole attached to cyano, C=N, C-NH<sub>2</sub> and carbonyl group. Enaminonitrile derivative **5** underwent acetylation when heated with acetic anhydride for one hour under reflux condition to obtain acetanilide pyrazole derivative containing adamantane moiety **6**. The IR spectrum of acetanilide pyrazole derivative **6** revealed signals at  $\nu$  3258 and broad 1694 cm<sup>-1</sup> related to NH and two carbonyl. <sup>1</sup>H NMR spectrum showed significant two signals at  $\delta$  8.27 and 10.69 ppm for pyrazole-H and NH of acetanilide exchangeable by D<sub>2</sub>O, while <sup>13</sup>C NMR displayed two singlet signals at  $\delta$  168.78 and 178.98 ppm for two carbonyl groups as well as signal for (C-NH) at  $\delta$  162.39 and adamantane carbons.

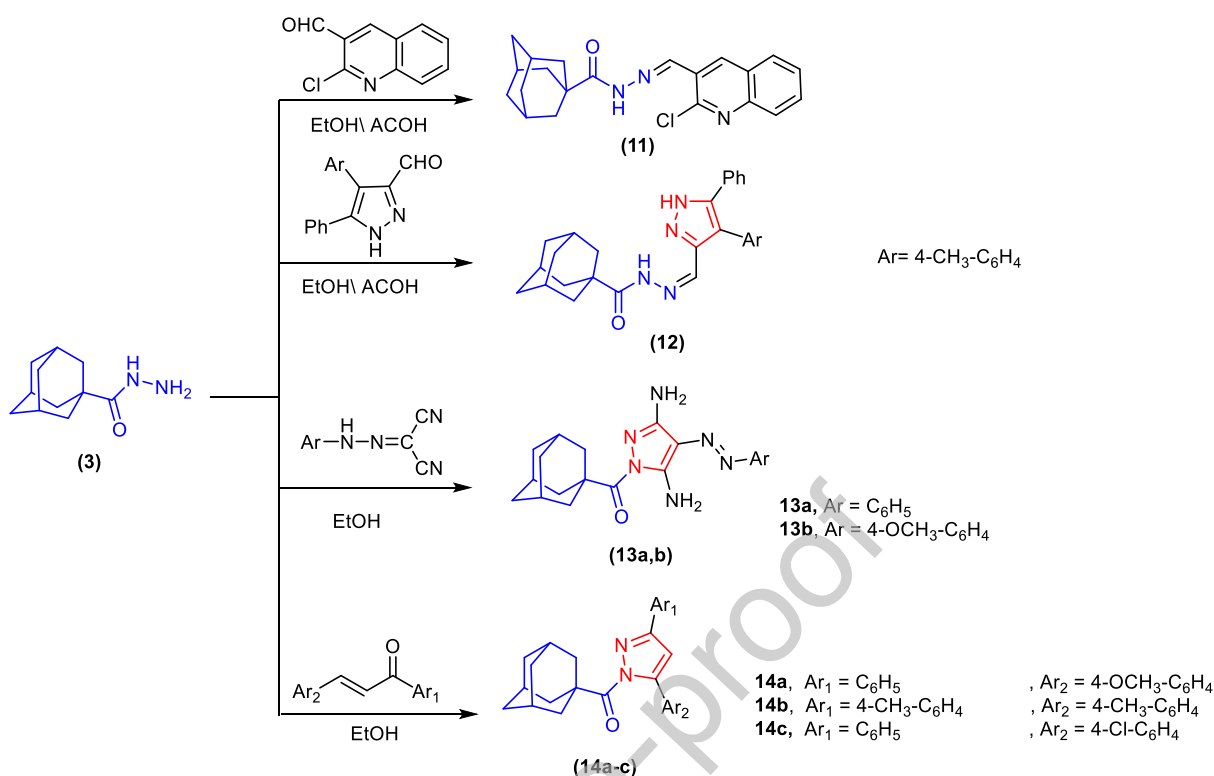


**Scheme 1:** Synthesis of 2-amino pyrazole and hydrazone derivatives containing adamantane pharmacophore

Similarity, the reaction of hydrazone derivative **3** with ethoxy methylene ethyl-cyanoacetate not demonstrate pyrazole derivatives as previous compounds **4**, **5** but the mechanism stops in addition elimination step and **not underwent cyclization to give** hydrazone derivative containing 2-cyanoacrylate and adamantane moiety **7**. **The IR spectra** of compound **7** showed absorption bands at  $\nu$  3246, 2213, 1710 and 1671  $\text{cm}^{-1}$  corresponding to NH, CN and carbonyl group. While,  $^1\text{H}$  NMR spectrum observed triplet and quartet signals at  $\delta$  1.34 and 4.26 with coupling constant ( $J = 6.7$  Hz) besides, three singlet signals at  $\delta$  2.28, 7.31 and 8.09 ppm for CH-vinylc and 2NH that

exchangeable by D<sub>2</sub>O added to three signals at  $\delta$  1.74-1.77, 1.91 and 2.09 ppm belonged to adamantane protons.

In the same way, the reactivity of hydrazide derivative **3** toward some electrophiles were checked as 1,3-dicarbonyl derivatives, and some heterocyclic bioactive core that is containing formyl derivatives as 2-chloro-3-formyl-quinoline and 5-phenyl-4-(*p*-tolyl)-1*H*-pyrazole-3-carbaldehyde and both don't undergo cyclization and produce acyclic hydrazone derivatives **9a-c**, **11** and **12** depending on characterization data. The IR spectrum of compound **9c** revealed stretching signals for NH and two carbonyl groups at  $\nu$  3236, 1678 and 1728 cm<sup>-1</sup>. The <sup>1</sup>H NMR spectrum of compound **9c** distinguished triplet and quartet signals, at  $\delta$  1.25, 3.70 ppm for ethyl group in addition to, five singlet signals at  $\delta$  1.72, 1.90, 1.91, 2.06 and 8.62 ppm related to adamantane protons, methyl and NH proton that exchangeable by D<sub>2</sub>O respectively. While <sup>1</sup>H NMR spectrum of compound **11** exhibited three singlet signals at  $\delta$  6.02, 8.45 and 8.66 ppm for NH, CH-methylinic and quinoline hydrogen, as well as two triplets and two doublet signals at  $\delta$  7.37, 7.66, 7.77 and 7.82 ppm associated to aromatic protons with coupling constant 7.5, 7.7, 8.0 and 8.4 Hz respectively. <sup>13</sup>C NMR spectrum of compound **9c** displayed signals for adamantane ranged between  $\delta$  27.66 to 40.05 ppm. Besides, three singlet signals two of them for the ethoxy group at  $\delta$  14.12, 61.53 ppm and the third signal at  $\delta$  58.45 ppm for methylene group as well as, three signals at  $\delta$  147.17, 165.03 and 173.47 for C=N and two carbonyl groups.



**Scheme (2):** Reaction of adamantane-1-carbohydrazide with some hetero aldehyde, azo aryldine and chalcone derivatives

As shown in **Scheme 2**, Pyrazole derivatives having an azo moiety were synthesized by the reaction of hydrazide derivatives **3** that coupled with *N*-phenyl hydrazonoyl malononitrile in the presence of ethanol and produced the corresponding **diamino-pyrazole 13a,b**. The structure of **compound 13a,b** pyrazole derivatives were confirmed with the help of analytical and spectroscopic data. Thus, the IR spectrum of **13a** exhibited stretching significance absorption bands at  $\nu$  3543, 3480, 3332 and 3281 cm<sup>-1</sup> for two amino groups and 1663 cm<sup>-1</sup> for carbonyl group. Its <sup>1</sup>H NMR spectrum of compound **13a** revealed three singlet signals between  $\delta$  1.77-2.03 ppm for adamantyl protons, two singlet signals at  $\delta$  6.13, 8.82 ppm for two amino groups exchangeable with D<sub>2</sub>O as well as five aromatic protons between  $\delta$  7.27-8.00 ppm. <sup>13</sup>C NMR spectrum of **compound 13b** exhibited signals for adamantane ranged between  $\delta$  28.05 to 39.37 ppm, in addition to, two singlet signals at  $\delta$  55.85 and  $\delta$  178.77 related to methoxy and carbonyl groups respectively. Moreover, signals for carbon attached to methoxy and amino groups at  $\delta$  159.86 and  $\delta$  147.64 as well as aromatic signals between  $\delta$  112.30-122.41 ppm.

Finally, **carbohydrazide derivative 3** was heated under reflux condition with  $\alpha,\beta$ -unsaturated carbonyl compound (chalcone) and furnished the corresponding pyrazole containing two arylidene groups at position three and five **14a-c**. The postulated structures of the newly designed pyrazole derivatives **were confirmed based on** elemental analysis and spectral data. IR spectrum of compound **14a** showed stretching characteristic bands at  $\nu$  1655  $\text{cm}^{-1}$  for carbonyl groups.  $^1\text{H}$  NMR spectrum of compound **14c** demonstrated singlet signal at  $\delta$  8.70 ppm for CH-pyrazole proton as well as adamantane and aromatic protons.  $^{13}\text{C}$  NMR spectrum of **14c** exhibited signals for adamantane in region  $\delta$  25.77-36.60 ppm, aromatic carbon between  $\delta$  114.84-143.73 ppm and three singlet signals at  $\delta$  144.08, 176.79, 188.91 ppm for C=C, C=N and carbonyl groups respectively.

## 3.2. Biological evaluation

### 3.2.1. Anti-proliferative activity

The *in vitro* cytotoxic activity of the new fourteen compounds that containing adamantane as an important pharmacophore backbone on different three cell lines, namely human breast adenocarcinoma cell line (MCF-7), human hepatocellular carcinoma cell line (HepG-2), as well as human lung adenocarcinoma epithelial cells (A549), were evaluated by using sulforhodamine B (SRB) assay according to reported methods [54,55]. Doxorubicin was used as a positive control and the obtained data represented in **table 1** as  $\text{IC}_{50}$  values expressed in  $\mu\text{M}$ .

The newly designed compounds in scheme **1** and **2** observed two mainly products as pyrazole derivatives (**4**, **5**, **6**, **12**, **13a-b** and **14a-c**) and hydrazone derivatives (**9a-c** and **11**) with only one hydrazine derivative compound **7** as well as the main bioactive core adamantane nucleus. **Most of the designed and** synthesized derivatives exhibited moderate to good activity against the tested cancer cell lines. In general, the tested compounds exhibited more sensitive and selectivity to lung cancer cells (A549) with  $\text{IC}_{50}$  values ranged between  $1.55 \pm 0.08$  to  $15.42 \pm 1.4 \mu\text{M}$ , with eight compounds (**4**, **5**, **9a**, **9b**, **9**, **12**, **13a** and **14c**) having  $\text{IC}_{50}$  less than or equal ten micromoles, except compound **14a** that showed  $\text{IC}_{50}$  ( $27.18 \pm 1.95 \mu\text{M}$ ) in comparison to **Dox**orubicin ( $\text{IC}_{50} = 2.58 \pm 0.03 \mu\text{M}$ ) rather than breast cancer (MCF-7) and liver cancer cells (HepG-2). At the same time, the tested compounds revealed activity against **HepG-2** with  $\text{IC}_{50}$  between ( $2.7 \pm 0.15$  to  $38.12 \pm 2.3 \mu\text{M}$ ) with five compounds less than  $\leq 10 \mu\text{M}$  and (MCF-7) displayed  $\text{IC}_{50}$  between ( $4.68 \pm 0.25$  to  $42.17 \pm 2.58 \mu\text{M}$ ) with only four compound  $\leq 10 \mu\text{M}$

compared to **Doxorubicin** for both cancer cells (  $11.46 \pm 0.95$  and  $15.29 \pm 1.2$   $\mu\text{M}$ ) respectively. From **table 1**, it's observed that four compounds (**9a**, **9c**, **12** and **13a**) exhibited promising and broad activity to all cell lines.

**Table 1:** IC<sub>50</sub> values expressed in ( $\mu\text{M}$ ) of the newly designed compounds against three cell lines

Cpd. No.	IC <sub>50</sub> %( $\mu\text{M}$ ) $\pm$ S.E*		
	MCF-7	HepG-2	A549
<b>4</b>	$12.45 \pm 0.97$	$9.31 \pm 0.82$	$8.4 \pm 0.75$
<b>5</b>	$15.54 \pm 1.46$	$13.89 \pm 1.2$	$10.57 \pm 0.86$
<b>6</b>	$23.45 \pm 1.75$	$18.21 \pm 1.61$	$13.46 \pm 1.08$
<b>7</b>	$35.13 \pm 2.45$	$28.17 \pm 1.9$	$15.42 \pm 1.4$
<b>9a</b>	$8.35 \pm 0.74$	$7.82 \pm 0.64$	$4.39 \pm 0.35$
<b>9b</b>	$20.64 \pm 1.8$	$12.48 \pm 1.1$	$10.78 \pm 0.86$
<b>9C</b>	$11.28 \pm 0.92$	$8.72 \pm 0.74$	$5.06 \pm 0.43$
<b>11</b>	$24.19 \pm 1.85$	$22.71 \pm 1.74$	$14.5 \pm 1.2$
<b>12</b>	$7.46 \pm 0.54$	$5.11 \pm 0.45$	$3.75 \pm 0.26$
<b>13a</b>	$4.68 \pm 0.25$	$2.7 \pm 0.15$	$1.55 \pm 0.08$
<b>13b</b>	$13.77 \pm 1.1$	$14.95 \pm 1.25$	$11.5 \pm 0.95$
<b>14a</b>	$42.17 \pm 2.58$	$38.12 \pm 2.3$	$27.18 \pm 1.95$
<b>14b</b>	$17.32 \pm 1.5$	$13.55 \pm 1.1$	$11.73 \pm 0.95$
<b>14c</b>	$15.29 \pm 1.2$	$11.46 \pm 0.95$	$8.52 \pm 0.65$
<b>Dox.</b>	$8.19 \pm 0.72$	$7.46 \pm 0.12$	$3.58 \pm 0.03$

- Each concentration was performed three times.

### 3.2.2. Structure activity relationship study

The activity of the synthesized compounds varies with respect to substitutions where the presence of pyrazole derivatives containing enaminonitrile as compounds **4** and **5** displayed activity to all cell lines, but the presence of (S-Me) in the ring of pyrazole in compound **4** observed higher activity than its analogue **5** with IC<sub>50</sub> (  $12.45 \pm 0.97$ ,  $9.31 \pm 0.82$  and  $8.4 \pm 0.75$   $\mu\text{M}$ ) and (  $15.54 \pm 1.46$ ,  $13.89 \pm 1.2$  and  $10.57 \pm 0.86$   $\mu\text{M}$ ) against MCF-7, HepG-2 and A549 respectively. Also, acetylation of the amino group in pyrazole enaminonitrile derivatives **5** failed to increase activity with IC<sub>50</sub> (  $23.45 \pm 1.75$ ,  $18.21 \pm 1.61$  and  $13.46 \pm 1.08$   $\mu\text{M}$ ) compared to

other derivatives **4**, **5** and **Doxorubicin**. Replacement enamionitrile pyrazole derivatives **4-6** with 3,5-diaminopyrazole **13a,b** or 3,5-diarylpyrazole derivatives **14a-c** exhibited that the presence of diamino as well as azo derivatives in position four in pyrazole enhance activity against all cell lines and among them azo-phenyl derivative **13a** demonstrated higher activity than azo-anisidine derivative **13b** with  $IC_{50}$  values for **13a,b** ( $4.68 \pm 0.25$ ,  $2.7 \pm 0.15$ ,  $1.55 \pm 0.08 \mu\text{M}$ ) and ( $13.77 \pm 1.1$ ,  $14.95 \pm 1.25$ ,  $11.5 \pm 0.95 \mu\text{M}$ ) against MCF-7, HepG-2 and A549 and in comparison to **Doxorubicin** ( $8.19 \pm 0.72$ ,  $7.46 \pm 0.12$ ,  $3.58 \pm 0.03 \mu\text{M}$ ) respectively.

Furthermore, the structure-activity relationships of a series of hydrazone derivatives were designed and tested on the same conditions. Adamantane-1-carbohydrazone derivatives **9a-c** showed that hydrazone of 3-methylacetylacetone **9a** and ethyl acetoacetate derivative **9c** displayed inhibitory activity higher than benzoyl acetone derivative **9b**. The presence of three methyl groups in hydrazono-3-methylpentan-2-one derivatives **9a** explored promising activity than one methyl and one phenyl as **9b** as well as compound **9c** that have one methyl and one ethoxy group and therefore  $IC_{50}$  values of hydrazone derivative **9a** ( $8.35 \pm 0.74$ ,  $7.82 \pm 0.64$ , and  $4.39 \pm 0.35 \mu\text{M}$ ) closely near to **Doxorubicin**. Additionally, hydrazine derivative **7** with adamantane as the backbone and acrylate derivative that poses two functional groups as ethyl ester and cyano groups displayed weak activity with almost  $IC_{50}$  values ranged between ( $15.42 \pm 1.4$  to  $35.13 \pm 2.45 \mu\text{M}$ ). To our delight, hydrazone containing pyrazole moiety (hybridization of two active core), compound **12** exhibited broad activity with  $IC_{50}$  values ( $7.46 \pm 0.54$ ,  $5.11 \pm 0.45$  and  $3.75 \pm 0.26 \mu\text{M}$ ) with  $IC_{50}$  values higher than **Doxorubicin** with 1.1 and 1.45 folds against MCF-7 and HepG-2.

Finally, based on the above analysis of SAR study, we can conclude that presence of pyrazole with diamino, and the azo-phenyl group as compound **13a**, hydrazone derivative by reaction with formyl pyrazole as compound **12** or with 3-methyl acetylacetone **9a** enhance the activity among all the designed compounds. As well as, the most promising synthesis 3,5-diaminopyrazole derivatives **13a** demonstrated  $IC_{50}$  values ( $4.68 \pm 0.25$ ,  $2.7 \pm 0.15$ ,  $1.55 \pm 0.08 \mu\text{M}$ ) with 1.75, 2.75 and 2.31 folds in comparison to all synthesized compounds and **Doxorubicin** as a positive control.

### 3.2.3. Carbonic anhydrase inhibitors

Carbonic anhydrase (CA) involved many isozymes that distributed to almost all organelle of the human body, and they are necessary for diversities of cellular mechanisms [62]. Inhibition of these isozymes is utilized to address an extensive range of disease situations containing glaucoma to cancer [63,64]. Both CA IX and CA XII become an important target for lung cancer drugs because it played a vital role in hypoxic condition by controlling intracellular and extracellular pH as well as, they are expressed in a limited number of normal tissues, so inhibition these two isoforms may have interesting clinical implications [56]. The modification of new CA inhibitors has been required to develop as therapeutic agents by introducing several groups as sulfonamide [65], thiourea derivatives [66], pyrazole derivatives [67], and bromophenols [68].

**Table 2:** Inhibitory activity of adamantane derivatives **9a**, **12** and **13a** on tumor associated carbonic anhydrase CAIX and CAXII

Cpd. No.	Carbonic anhydrase	
	CA IX	CA XII
<b>9a</b>	256.32 ± 3.3	527.86 ± 7.8
<b>12</b>	217.78 ± 4.2	252.25 ± 5.4
<b>13a</b>	85.75 ± 1.4	144.16 ± 2.5
Acetazolamide	41.53 ± 0.7	68.75 ± 1.2

\*Three independent measurements were performed for each used concentration of the tested compounds.

Depending on the antiproliferative activity results, it found that the most adamantane derivatives exhibited selectivity to lung cancer cell line A549. Among them, we selected the most potent three compounds **9a**, **12** and **13a** ( $IC_{50}$  values less than  $5\mu M$ ) to further evaluation against *in vitro* CA IX and CAXII. The data obtained was represented in **table 2**, by inhibitory constants  $K_{IS}$  in (nM) according to 4-nitrophenyl acetate (4-NPA) esterase assay and Acetazolamide used as a standard inhibitor drug.

From the inhibitory efficiency that represented in **table 2**, it found that the three adamantane derivatives exhibited good inhibitory activity against two isoenzymes CAIX and CA XII by

displaying activity in small micromole between (0.085-0.527 $\mu$ M). Firstly, 3,5-diaminoazopyrazole derivative **13a** was the most active derivative and had a significant inhibitory effect against both **two isoenzymes** CAIX and CA XII with  $K_I$  values  $85.75 \pm 1.4$  and  $144.16 \pm 2.5$  (nM), in comparison to Acetazolamide that revealed  $IC_{50}$  values ( $41.53 \pm 0.7$  and  $68.75 \pm 1.2$  nM) respectively. Furthermore, the combination between pyrazole and adamantane-1-carbohydrazide to produce **hydrazone derivative 12** with adamantane core showed moderate activity on CAIX with reduce  $K_I$  values  $217.78 \pm 4.2$  (nM) and  $252.25 \pm 5.4$  (nM) for CAXII and that illustrate that combination of the formyl pyrazole with hydrazine derivative decrease activity. On the other hand, testing of adamantane hydrazone derivative that obtained by incorporation of adamantane hydrazide moiety with 3-methyl acetylacetone without any pyrazole core as adamantane derivative **9a** arose as **the weakest CA derivative** in this study with  $K_I$  values  $256.32 \pm 3.3$  and  $527.85 \pm 7.8$  (nM) against CAIX and CA XII respectively (**Fig.2**).

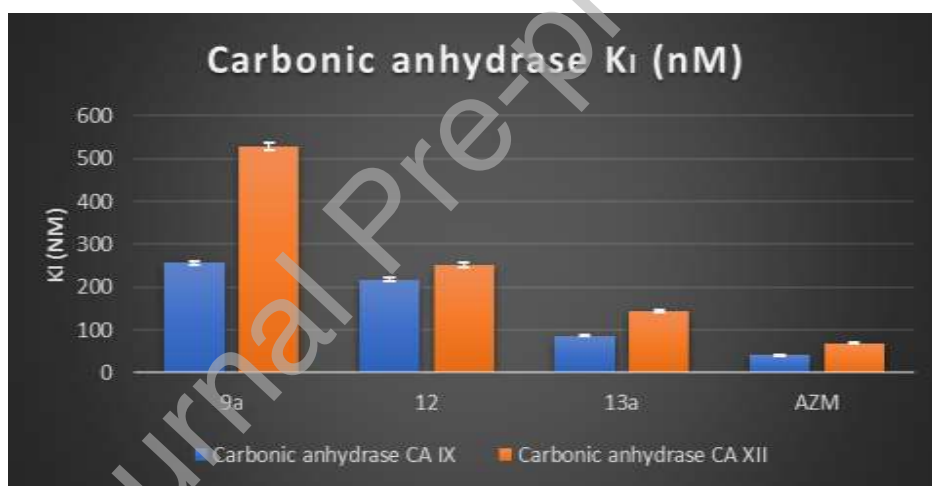


**Figure 2:** Diagram illustrates the inhibitory efficiency  $K_I$  (nM) of adamantane derivative **9a**, **12**, **13a** and Acetazolamide against transmembrane CA IX and CA XII

Finally, it can conclude that the adamantane derivatives exhibited potency activity to lung adenocarcinoma A549 with  $IC_{50}$  values in low micromoles in general, but only adamantane **derivatives that having pyrazole** moiety without any hydrazone part in the main skeleton exhibited a good activity to carbonic anhydrase IX and XII, and its noteworthy to mention the order of activity within pyrazole (**13a**) > pyrazole-hydrazone derivative (**12**) > hydrazone derivatives (**9a**) and all containing bioactive adamantane core

### 3.2.4. *In silico* Computational studies

#### 3.2.4.1. Predication of the Drug likeness and physicochemical properties

Physicochemical properties can be defined as the interaction of a new compound or drug with the physical environment and used to determine both the proper formulation and delivery method of a drug [69]. The three adamantane derivatives **9a**, **12** and **13a** that tested against CA IX and CA XII were evaluated by using Swiss ADME (<http://swissadme.ch/index.php>) for physicochemical properties and two drug-likeness rule (Lipinski's and Veber rule) [70]. The adamantane derivative that having hydrazone **9a**, and diamino-pyrazole derivative **13a** showed oral bioavailability without any violations for both Lipinski's Rule according to reported methods [47,49,51] that discussed in details and summarized in table 3 and Veber filter [71] that include two-parameter that can be known as (i) number of rotatable bonds less than or equal 10 and (ii) topological polar surface area (TPSA) less than or equal  $140 \text{ \AA}^2$ . Except hydrazone-pyrazole derivative **12** that displayed only one violation  $MLOGP > 4.15$ , but all the tested compounds, as well as two standard drugs, meet the criteria of drug-likeness. while the two standard drugs failed in Veber filter where  $TPSA > 140$ .

**Table 3:** *In silico* the physicochemical properties and Lipinski's rule of five and Veber filter for the adamantane derivatives **9a**, **12**, **13a** and Acetazolamide (AZM) as a positive control

Cpd.							Violations	Violations
No.	MW	MLogP	nHBA	nHBD	nRB	TPSA	from Lipinski's	from Veber filter
Rule	<500	≤4.15	≤10	≤5	≤10	≤140 $\text{\AA}^2$	Yes; 0 or 1 violation	Yes; 0 violation
<b>9a</b>	290.40	2.52	3	1	5	58.53	Yes; 0 violation	Yes; 0 violation
<b>12</b>	438.56	4.27	7	2	6	70.14	Yes; 1 violation: MLogP	Yes; 0 violation
<b>13a</b>	364.44	3.50	4	2	4	111.65	Yes; 0 violation	Yes; 0 violation
<b>AZM</b>	222.25	-2.34	6	2	3	151.66	Yes; 0 violation	No; 1 violation: TPSA>140

### 3.2.4.2. Molecular docking study

Molecular docking simulation considered the simplified form of molecular dynamic (MD) simulation that save time and money spent and common component of the drug discovery because traditional experimental methods for drug discovery take a long time [72,73]. Docking study can also be defined as a computational procedure that studies how ligand and protein fit both energetically and geometrically to give us a complete figure to predict the binding-conformation of small drug-like molecules to target proteins [74,75]. To provide a rationale for the cytotoxic activity and carbonic anhydrase values of the newly adamantane derivatives **9a**, **12** and **13a**, the molecular docking simulation was performed using Molecular Operating Environment software 10.2008 (MOE) to predict the possible binding mode as well as the active conformation of these derivatives inside the target enzyme. The three compounds were docked in two proteins that retrieved from protein data bank (<https://www.rcsb.org/>) as **CA IX** (PDB: 3IAI) and **CA XII** (PDB: 1JD0) [56,57].

Firstly, the validation process inside the active site of **CA IX** (PDB: 3IAI) showed that the original ligand 5-acetamido-1,3,4-thiadiazole-2-sulfonamide that known as Acetazolamide (**AZM**) inhibitor fitted deeply inside the active side with (RMDS = 1.02 Å) and exhibited energy score  $S = -9.94$  Kcal/mol, and three hydrogen bond that can be described as one hydrogen bond acceptor between Thr200 between the oxygen of the sulphonamide with bond length 2.66 Å (strength= 96%). Besides, two hydrogen bonds donor with the nitrogen of sulfonamide group through a bond length of 2.77 Å (68%) and 3.24 Å (12%). The Zn ion that contacts one nitrogen of sulphonamide and three amino acids residue as His 119, 96, 94 (supplementary information). (**Fig. 3**).

Then the promising derivatives **9a**, **12**, and **13a** were docked inside the active site of **CA IX** (PDB: 3IAI). Docking of hydrazone-adamantane derivatives **9a** showed binding energy  $S = -10.96$  Kcal/mol and formed only one hydrogen bond acceptor with His 64 with bond length 2.80 Å (14%). Besides, the carbonyl of hydrazone side chain bound to  $Zn^{+2}$  ion by coordinate bond as well as  $Zn^{+2}$  ion surrounded by three coordinated bonds with His 119, 96 and 94 as the original ligand (**AZM**) (**Fig. 4**). By the same way, pyrazolo-hydrazone derivatives **12** (**Fig. 5**) demonstrate one side chain hydrogen bond donor between Gln92 and NH of pyrazole with

strength (12%) and bond length (2.95 Å) (See **table 4**). Furthermore, arene-cation interaction between tolyl of pyrazole derivative and His64 added to arene-arene cation interaction between His94 and phenyl ring at position five in pyrazole derivatives and these binding exhibited binding energy  $S = -12.63$  Kcal/mol. Compound **13a** with  $K_I$  values against CA IX ( $85.75 \pm 1.4$  nM) advertised binding energy  $S = -9.94$  Kcal/mol with one hydrogen bond acceptor through His64 and carbonyl of methanone adamantane derivative with bond length 2.51 Å (40%), beside  $Zn^{+2}$  ion form arene-cation interaction with phenyl of the azo-pyrazole derivative. Adamantane moiety in all previous pose showed lipophilic interaction with the carbonic anhydrase binding site.

**Table 4:** Docking results of the promising adamantane derivatives **9a**, **12**, and **13a** inside 3IAI and 1JD0 active site

Cpd. No.	(S) (Kcal/mol)	Interacting residues	Type of interaction
<b>For CAIX (3IAI)</b>			
<b>AZM</b>	-9.94	Thr199 Thr200, His94 and [His94, His96, His119(Zn)*]	H-bond
<b>9a</b>	-10.96	His64, His96 and [His94, His96, His119 (Zn)*]	H-bond
<b>12</b>	-12.63	Gln92, His64 and His94	H-bond & aren-cation aren-arene
<b>13a</b>	-9.94	His96	H-bond & aren-cation
<b>For CAXII (1JD0)</b>			
<b>AZM</b>	-11.55	Thr199, Thr200, His94, His119 and [His94, His96, His119(Zn)*]	H-bond
<b>9a</b>	-14.31	His96 and [His94, His96, His119(Zn)*]	H-bond
<b>12</b>	-12.81	Lys 67	H-bond & aren-cation
<b>13a</b>	-13.87	His94, Thr91	H-bond & aren-cation aren-arene

(\*) meaning that Zn ion bind to ligand and the residue amino acid.

Self-docking of **Acetazolamide** inside the active site of (PDB: 1JD0) to perform the validation process displayed binding energy  $S = -11.55$  Kcal/mol and formed many binding bonds as amino

acid residue Thr199 formed one Hydrogen bond backbone acceptor with the oxygen of sulfonamide with bond length 2.66 Å (79%) as well as another hydrogen bond side chain donor with a nitrogen of sulfonamide group with bond length 2.59 Å (83%). In the same way, both His 119 and His94 formed two hydrogen bond side chain donors with the nitrogen of sulfonamide with bond length 2.74 Å (20%) and 3.37 Å (11%), respectively. Also, Thr200 bind with two nitrogen of thiadiazole of acetazolamide with two hydrogen bonds acceptor with a bond length of 3.20 Å (15%) and 2.48 Å (27%). The Zn ions bound to the nitrogen of sulfonamide and formed three coordinate bonds with amino acids (His94, His96, and His119) beside vital water molecule that contact with the nitrogen of acetanilide of acetazolamide and nitrogen of thiadiazole as well as two amino acids Thr200 and Pro201. (**Fig. 6**).

Furthermore, compound **9a** that have hydrazone derivatives, His96 (hydrogen bond acceptor 3.15Å) and Zn ion bind with oxygen of the carbonyl by coordinate bond and the same three histidine amino acid as a ligand with binding energy  $S = -14.31$ Kcal/mol as well as hydrophobic interaction between adamantane moiety and two methyl groups with the active site of pocket (**Fig. 7**). Also, pyrazole derivative **12** with inhibitory efficiency 0.252  $\mu$ M showed the lowest binding energy  $S = -12.81$ Kcal/mol, where His 94 form one hydrogen bond acceptor (2.87 Å) with the carbonyl of the adamantane carbohydrazone derivatives and one arene-cation interaction with tolyl of pyrazole derivatives. Pyrazole derivative **13a** with two amino (in position 3 and 5) and azo-phenyl (position 4) derivative observed a lower docking score energy binding energy  $S = -13.87$  Kcal/mol. Moreover, it formed hydrogen bond acceptor (2.57Å and 42%) between the carbonyl of methanone derivative and Thr91 and one arene-arene interaction between phenyl and His94 as well as one arene-cation interaction through the pyrazole ring and Lys 67 (**Fig. 8**). (supplementary data containing all figure).

Finally, the presence of pyrazole derivative enhances binding affinity because it can form many different interactions, as well as the presence of carbonyl at a side chain or tightly direct to pyrazole ring also, increase binding inside the pock in addition, it can bind to Zn ion, and presence of adamantane core (lipophilic properties) exhibited hydrophobic interaction with the active site in a pocket.

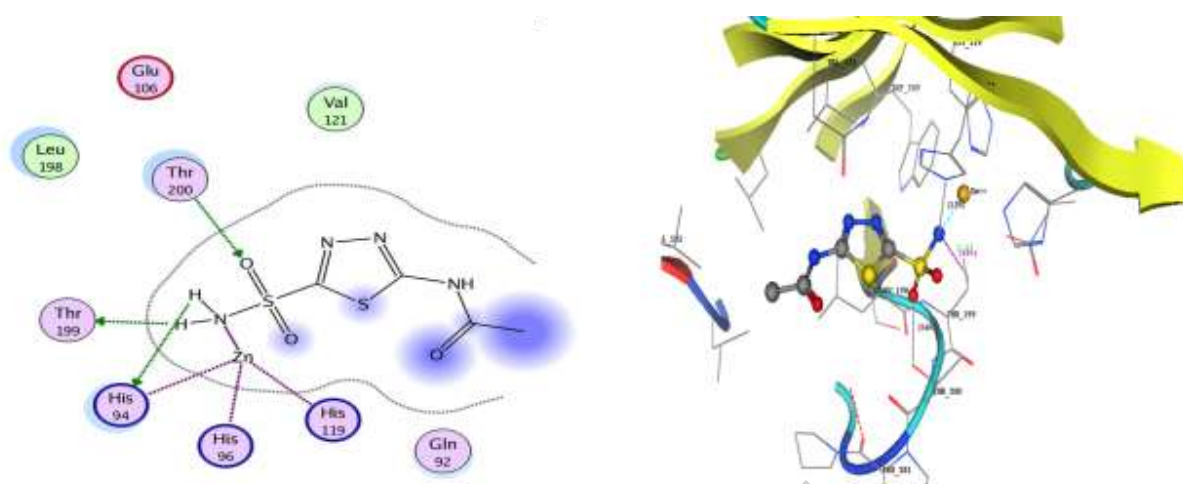


**Figure 3:** 2D &3D interactions of Acetazolamide(AZM) inhibitor in the active site of 3IaI (CA IX)

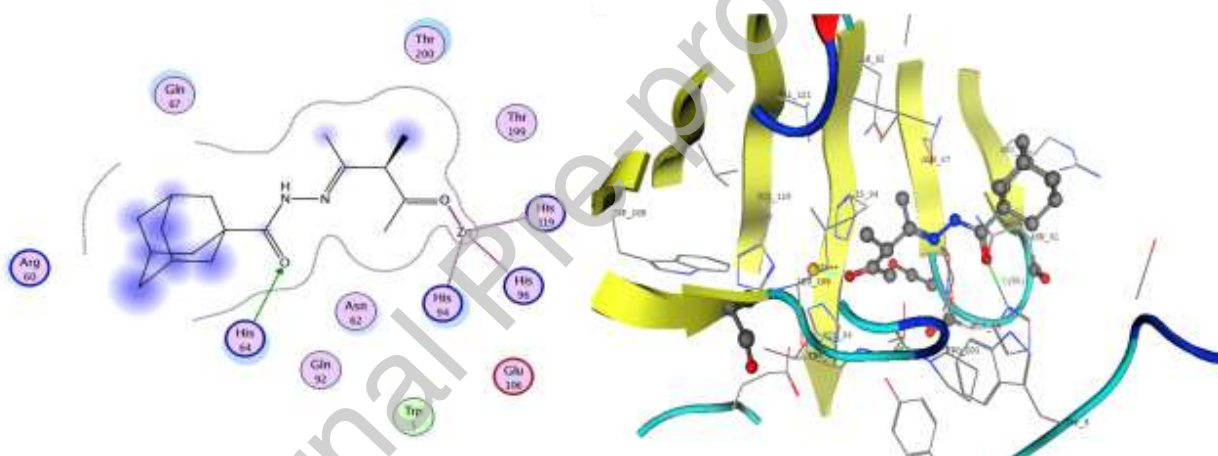


**Figure 4:** 2D &3D interactions of compound 9a in the active site of 3IaI (CA IX)

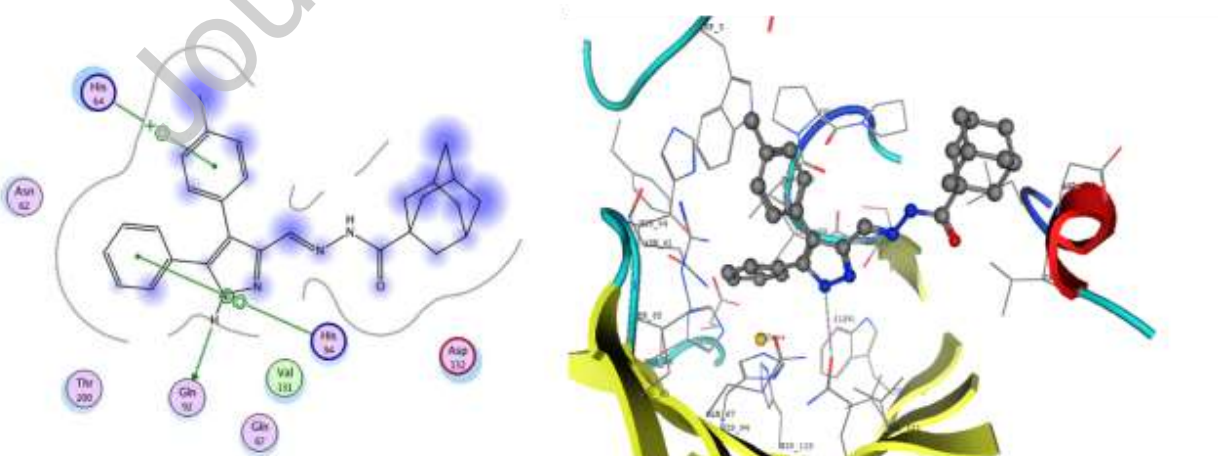


**Figure 5:** 2D &3D interactions of compound 12 in the active site of 3IaI (CA IX).

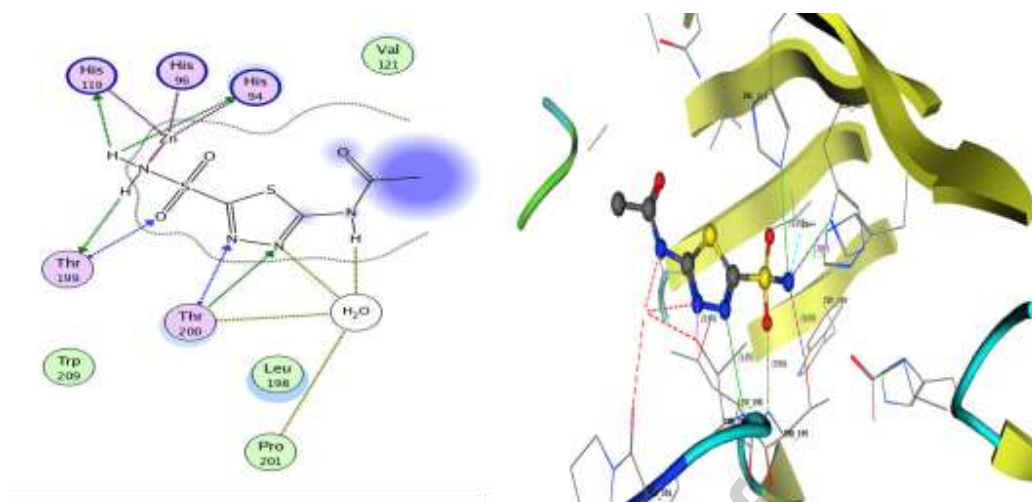


**Figure 6:** 2D &3D interactions Acetazolamide (AZM) in the active site of 1JD0 (CA XII)

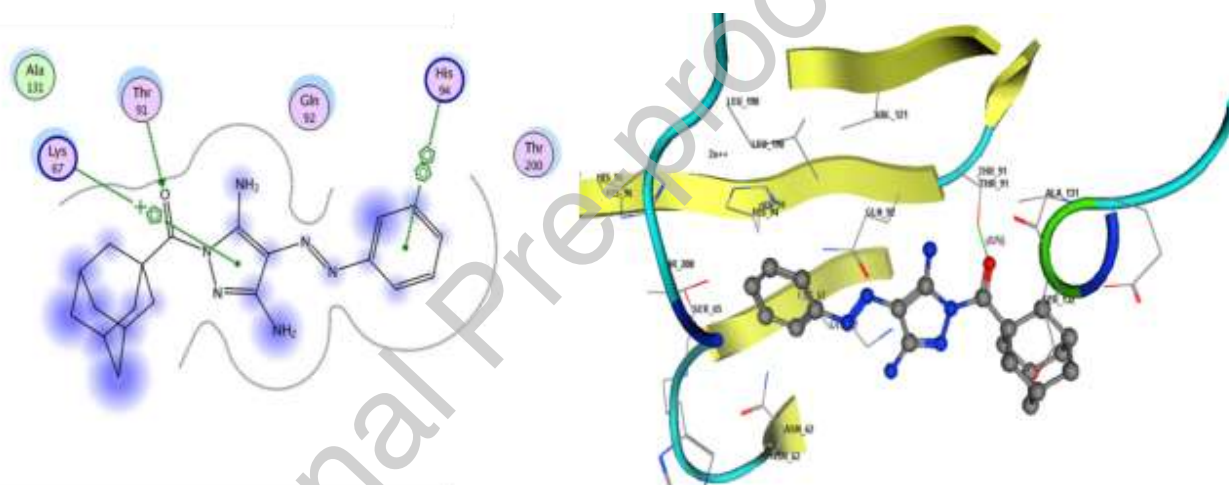


**Figure 7:** 2D &3D interactions of compound 12 in the active site of 1JD0 (CA XII).

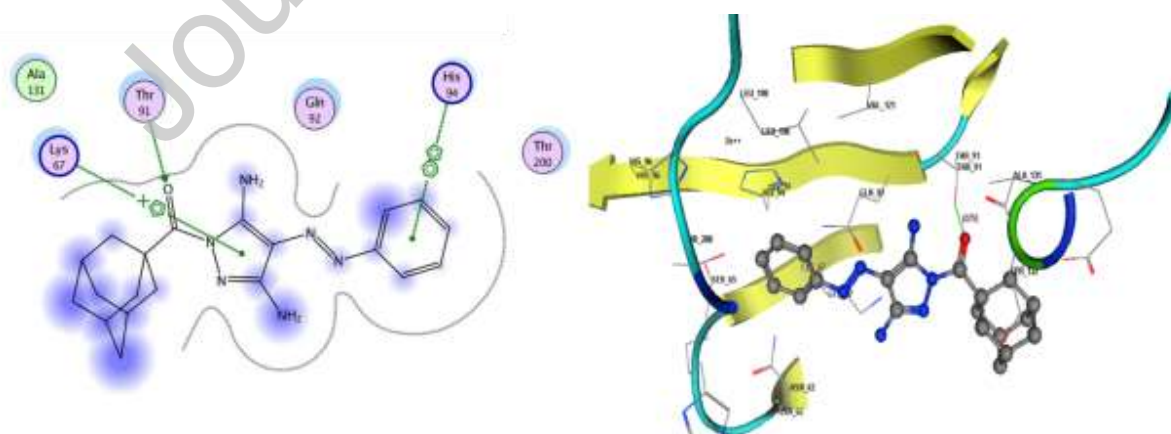


**Figure 8:** 2D &3D interactions of compound 13a in the active site of 1JD0 (CA XII)

#### 4. Conclusion

Generally, we successfully designed and synthesized a small library of adamantane nucleus (lipophilic part) bearing pyrazole **4**, **5**, **6**, **12**, **13**, **14**, and hydrazone **7**, **9**, **11** derivatives at **position one** and all the chemical reaction involve an only one-step reaction to obtain the desired products. The cytotoxic activity against three cell line MCF-7, HepG-2 and A549 were evaluated and displayed good to moderated activity with  $IC_{50}$  values (1.55-42.17  $\mu$ M). The newly synthesized derivatives revealed sensitive and selectivity to lung cancer cells (A549) with  $IC_{50}$  values ranged between  $1.55 \pm 0.08$  to  $15.42 \pm 1.4$   $\mu$ M, with eight compounds (**4**, **5**, **9a**, **9b**, **9c**, **12**, **13a** and **14c**) having  $IC_{50}$  less than or equal ten micromole except for compound **14a** that showed  $IC_{50}$  ( $27.18 \pm 1.95$   $\mu$ M). The most promising three adamantane derivatives **9a**, **12** and **13a** with  $IC_{50}$  values less than 5  $\mu$ M were elected to evaluate their inhibitory action against isoenzyme hCAIX and hCAIXII for the first time. Additionally, 3,5-diamino-pyrazole core **13a** showed higher  $K_I$  values than hydrazo-pyrazole **12** and hydrazone derivatives **9a** that hybrid with adamantane and exhibited inhibitory effect with submicromolar between (0.085-0.527  $\mu$ M), in comparison to **Acetazolamide** (0.041-0.068  $\mu$ M). Among them, compound **13a** is considered the most **promising derivative** with anti-proliferative (A549) ( $IC_{50} = 1.55 \pm 0.08$   $\mu$ M) and CAIX/XII inhibitors ( $K_I = 0.085$  and  $0.144$   $\mu$ M), respectively. Finally, some drug-likeness model as Lipinski and Verber were predicted. Molecular docking simulation was performed inside the active site of CA IX (PDB: 3IAI) and CA XII (PDB: 1JD0) to evaluate the binding modes of the adamantane derivatives as well as Acetazolamide. Docking score of the promising compounds showed lower values (-9.94 to -14.31 Kcal/mol) in comparison to Acetazolamide (-9.94 to -11.55 Kcal/mol) and different type of interaction as H-bond, arene-arene and arene-cation interaction were present beside in some cases ligand coordinated to Zn ion. Moreover, due to lipophilic characters of adamantane core the hydrophobic interaction appear with both active sites.

## Author statements

**Mohammed M. S. Wassel**; Conceptualization, Performed the experiments, Methodology, Investigation, Resources, Writing - Original Draft.

**Ahmed Ragab**; Conceptualization, Methodology, Software, Formal analysis, Validation, Methodology, Investigation, Data Curation, Writing - Original Draft, Writing Review & Editing, Visualization.

**Gameel A. M. Elhag Ali**; Conceptualization, Methodology, Resources, Writing - Original Draft, Supervision.

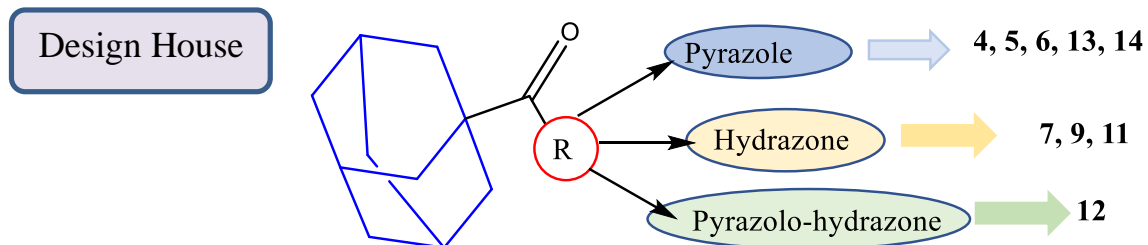
**Ahmed B. M. Mehany**; Performed the experiments for biological parts.

**Yousry A. Ammar**; Conceptualization, Methodology, Formal analysis, Investigation, Resources Writing Original Draft and Supervision.

## Conflicts of interest

The authors declare that they have no known competing financial interests or personal relationships that could have appeared to influence the work reported in this paper.

## Graphical abstract



Cpd. No.	Structure	Carbonic anhydrase $K_I$ (nM)*	
		CA IX	CA XII
9a		$256.32 \pm 3.3$	$527.86 \pm 7.8$
12		$217.78 \pm 4.2$	$252.25 \pm 5.4$
13a		$85.75 \pm 1.4$	$144.16 \pm 2.5$
AZM		$41.53 \pm 0.7$	$68.75 \pm 1.2$

A series of pyrazole and hydrazone containing adamantane was designed, synthesized and evaluated as *in vitro* an antiproliferative and carbonic anhydrase inhibitor.

## References

- [1] M.F. Khan, T. Anwer, A. Bakht, G. Verma, W. Akhtar, M.M. Alam, M.A. Rizvi, M. Akhter, M. Shaquiquzzaman, Unveiling novel diphenyl-1H-pyrazole based acrylates tethered to 1,2,3-triazole as promising apoptosis inducing cytotoxic and anti-inflammatory agents, *Bioorg. Chem.* 87 (2019) 667–678. doi:<https://doi.org/10.1016/j.bioorg.2019.03.071>.
- [2] M. Taha, S.A. Ali Shah, M. Afifi, M. Zulkeflee, S. Sultan, A. Wadood, F. Rahim, N.H. Ismail, Morpholine hydrazone scaffold: Synthesis, anticancer activity and docking studies, *Chinese Chem. Lett.* 28 (2017) 607–611. doi:<https://doi.org/10.1016/j.ccllet.2016.10.020>.
- [3] J.S. You, P.A. Jones, Cancer Genetics and Epigenetics: Two Sides of the Same Coin?, *Cancer Cell.* 22 (2012) 9–20. doi:<https://doi.org/10.1016/j.ccr.2012.06.008>.
- [4] C.-J. Liu, S.-L. Yu, Y.-P. Liu, X.-J. Dai, Y. Wu, R.-J. Li, J.-C. Tao, Synthesis, cytotoxic activity evaluation and HQSAR study of novel isosteviol derivatives as potential anticancer agents, *Eur. J. Med. Chem.* 115 (2016) 26–40. doi:<https://doi.org/10.1016/j.ejmech.2016.03.009>.
- [5] P. Wang, J. Cai, J. Chen, M. Ji, Synthesis and anticancer activities of ceritinib analogs modified in the terminal piperidine ring, *Eur. J. Med. Chem.* 93 (2015) 1–8. doi:<https://doi.org/10.1016/j.ejmech.2015.01.056>.
- [6] R.R. Ruddaraju, A.C. Murugulla, R. Kotla, M. Chandra Babu Tirumalasetty, R. Wudayagiri, S. Donthabakthuni, R. Maraju, K. Baburao, L.S. Parasa, Design, synthesis, anticancer, antimicrobial activities and molecular docking studies of theophylline containing acetylenes and theophylline containing 1,2,3-triazoles with variant nucleoside derivatives, *Eur. J. Med. Chem.* 123 (2016) 379–396. doi:<https://doi.org/10.1016/j.ejmech.2016.07.024>.
- [7] I. Chaaban, E.S.M. El Khawass, H.A. Abd El Razik, N.S. El Salamouni, M. Redondo-Horcajo, I. Barasoain, J.F. Díaz, J. Yli-Kauhaluoma, V.M. Moreira, Synthesis and biological evaluation of new oxadiazoline-substituted naphthalenyl acetates as anticancer agents, *Eur. J. Med. Chem.* 87 (2014) 805–813. doi:<https://doi.org/10.1016/j.ejmech.2014.10.015>.
- [8] F. Bray, J. Ferlay, I. Soerjomataram, R.L. Siegel, L.A. Torre, A. Jemal, Global cancer statistics 2018: GLOBOCAN estimates of incidence and mortality worldwide for 36

- cancers in 185 countries, CA. Cancer J. Clin. 68 (2018) 394–424. doi:10.3322/caac.21492.
- [9] M. Nagasaka, A. Lehman, R. Chlebowski, B.M. Haynes, G. Ho, M. Patel, L.C. Sakoda, A.G. Schwartz, M.S. Simon, M.L. Cote, COPD and lung cancer incidence in the Women's Health Initiative Observational Study: A brief report, Lung Cancer. 141 (2020) 78–81. doi:https://doi.org/10.1016/j.lungcan.2020.01.006.
- [10] L. Zhu, S. Huang, J. Li, J. Chen, Y. Yao, L. Li, H. Guo, X. Xiang, J. Deng, J. Xiong, Sophoridine inhibits lung cancer cell growth and enhances cisplatin sensitivity through activation of the p53 and Hippo signaling pathways, Gene. 742 (2020) 144556. doi:https://doi.org/10.1016/j.gene.2020.144556.
- [11] S.L. Parker, T. Tong, S. Bolden, P.A. Wingo, Cancer statistics, 1996, CA. Cancer J. Clin. 46 (1996) 5–27. doi:10.3322/canjclin.46.1.5.
- [12] J.F. Domsic, B.S. Avvaru, C.U. Kim, S.M. Gruner, M. Agbandje-McKenna, D.N. Silverman, R. McKenna, Entrapment of Carbon Dioxide in the Active Site of Carbonic Anhydrase II, J. Biol. Chem. . 283 (2008) 30766–30771. doi:10.1074/jbc.M805353200.
- [13] S. Bal, R. Kaya, Y. Gök, P. Taslimi, A. Aktaş, M. Karaman, İ. Gülçin, Novel 2-methylimidazolium salts: Synthesis, characterization, molecular docking, and carbonic anhydrase and acetylcholinesterase inhibitory properties, Bioorg. Chem. 94 (2020) 103468. doi:https://doi.org/10.1016/j.bioorg.2019.103468.
- [14] Y. Wang, H. Guo, G. Tang, Q. He, Y. Zhang, Y. Hu, Y. Wang, Z. Lin, A selectivity study of benzenesulfonamide derivatives on human carbonic anhydrase II/IX by 3D-QSAR, Molecular Docking and Molecular Dynamics Simulation, Comput. Biol. Chem. 80 (2019) 234–243. doi:https://doi.org/10.1016/j.compbiolchem.2019.03.005.
- [15] D. Tanini, L. Ricci, A. Capperucci, L. Di Cesare Mannelli, C. Ghelardini, T.S. Peat, F. Carta, A. Angeli, C.T. Supuran, Synthesis of novel tellurides bearing benzenesulfonamide moiety as carbonic anhydrase inhibitors with antitumor activity, Eur. J. Med. Chem. 181 (2019) 111586. doi:https://doi.org/10.1016/j.ejmech.2019.111586.
- [16] G. Bianco, R. Meleddu, S. Distinto, F. Cottiglia, M. Gaspari, C. Melis, A. Corona, R. Angius, A. Angeli, D. Taverna, S. Alcaro, J. Leitans, A. Kazaks, K. Tars, C.T. Supuran, E. Maccioni, N-Acylbenzenesulfonamide Dihydro-1,3,4-oxadiazole Hybrids: Seeking Selectivity toward Carbonic Anhydrase Isoforms, ACS Med. Chem. Lett. 8 (2017) 792–796. doi:10.1021/acsmchemlett.7b00205.

- [17] C.T. Supuran, Carbonic anhydrases-an overview, *Curr. Pharm. Des.* 14 (2008) 603–614.
- [18] L. Tang, Q. Zhao, S. Wu, J. Cheng, J. Chang, J.-T. Guo, The current status and future directions of hepatitis B antiviral drug discovery, *Expert Opin. Drug Discov.* 12 (2017) 5–15. doi:10.1080/17460441.2017.1255195.
- [19] S.J. Takate, A.D. Shinde, B.K. Karale, H. Akolkar, L. Nawale, D. Sarkar, P.C. Mhaske, Thiazolyl-pyrazole derivatives as potential antimycobacterial agents, *Bioorg. Med. Chem. Lett.* 29 (2019) 1199–1202. doi:https://doi.org/10.1016/j.bmcl.2019.03.020.
- [20] H. Kikuchi, B. Yuan, X. Hu, M. Okazaki, Chemopreventive and anticancer activity of flavonoids and its possibility for clinical use by combining with conventional chemotherapeutic agents, *Am. J. Cancer Res.* 9 (2019) 1517–1535. <https://pubmed.ncbi.nlm.nih.gov/31497340>.
- [21] J. Zhang, S. Wang, Y. Ba, Z. Xu, Tetrazole hybrids with potential anticancer activity, *Eur. J. Med. Chem.* 178 (2019) 341–351. doi:https://doi.org/10.1016/j.ejmech.2019.05.071.
- [22] C. Zhuang, X. Guan, H. Ma, H. Cong, W. Zhang, Z. Miao, Small molecule-drug conjugates: A novel strategy for cancer-targeted treatment, *Eur. J. Med. Chem.* 163 (2019) 883–895. doi:https://doi.org/10.1016/j.ejmech.2018.12.035.
- [23] M.S. Islam, C. Wang, J. Zheng, N. Paudyal, Y. Zhu, H. Sun, The potential role of tubeimosides in cancer prevention and treatment, *Eur. J. Med. Chem.* 162 (2019) 109–121. doi:https://doi.org/10.1016/j.ejmech.2018.11.001.
- [24] G. Hughes, M.A. Webber, Novel approaches to the treatment of bacterial biofilm infections, *Br. J. Pharmacol.* 174 (2017) 2237–2246. doi:10.1111/bph.13706.
- [25] M. Fesatidou, P. Zagaliotis, C. Camoutsis, A. Petrou, P. Eleftheriou, C. Tratrak, M. Haroun, A. Geronikaki, A. Ciric, M. Sokovic, 5-Adamantan thiazolidinone-based thiazolidinones as antimicrobial agents. Design, synthesis, molecular docking and evaluation, *Bioorg. Med. Chem.* 26 (2018) 4664–4676. doi:https://doi.org/10.1016/j.bmc.2018.08.004.
- [26] I. Blanco-Montenegro, R. De Ritis, M. Chiappini, Imaging and modelling the subsurface structure of volcanic calderas with high-resolution aeromagnetic data at Vulcano (Aeolian Islands, Italy), *Bull. Volcanol.* 69 (2007) 643–659. doi:10.1007/s00445-006-0100-7.
- [27] N.J. Vickers, Animal Communication: When I'm Calling You, Will You Answer Too?, *Curr. Biol.* 27 (2017) R713–R715. doi:https://doi.org/10.1016/j.cub.2017.05.064.

- [28] K.S. Rosenthal, M.S. Sokol, R.L. Ingram, R. Subramanian, R.C. Fort, Tromantadine: inhibitor of early and late events in herpes simplex virus replication., *Antimicrob. Agents Chemother.* 22 (1982) 1031 LP – 1036. doi:10.1128/AAC.22.6.1031.
- [29] Mi. Shchelkanov, V.A. Shibnev, I.T. Finogenova, T.M. Fediakina, T.M. Garaev, N. V Markova, I.M. Kirillov, The antiviral activity of the adamantane derivatives against the influenza virus A (H1N1) pdm2009 model in vivo, *Vopr. Virusol.* 59 (2014) 37–40.
- [30] J. McSharry, K. Zager, Q. Weng, D. Chernoff, G. Drusano, Pharmacodynamics of NPI-5291, an Adamantane Class Compound, for Influenza A Viruses, *Antiviral Res.* 3 (2007) A61.
- [31] T. Lampejo, Influenza and antiviral resistance: an overview, *Eur. J. Clin. Microbiol. Infect. Dis.* 39 (2020) 1201–1208. doi:10.1007/s10096-020-03840-9.
- [32] A.G. Ali, M.F. Mohamed, A.O. Abdelhamid, M.S. Mohamed, A novel adamantane thiadiazole derivative induces mitochondria-mediated apoptosis in lung carcinoma cell line, *Bioorg. Med. Chem.* 25 (2017) 241–253. doi:https://doi.org/10.1016/j.bmc.2016.10.040.
- [33] N. Basarić, M. Sohora, N. Cindro, K. Mlinarić-Majerski, E. De Clercq, J. Balzarini, Antiproliferative and Antiviral Activity of Three Libraries of Adamantane Derivatives, *Arch. Pharm. (Weinheim)*. 347 (2014) 334–340. doi:10.1002/ardp.201300345.
- [34] E.S. Al-Abdullah, H.M. Al-Tuwaijri, H.M. Hassan, M.A. Al-Alshaikh, E.E. Habib, A.A. El-Emam, Synthesis, Antimicrobial and Hypoglycemic Activities of Novel N-(1-Adamantyl)carbothioamide Derivatives, *Molecules*. 20 (2015) 8125–8143. doi:10.3390/molecules20058125.
- [35] L. Pellegatti, J. Sedelmeier, Synthesis of Vildagliptin Utilizing Continuous Flow and Batch Technologies, *Org. Process Res. Dev.* 19 (2015) 551–554. doi:10.1021/acs.oprd.5b00058.
- [36] M.A. Abou-Gharbia, W.E. Childers, H. Fletcher, G. McGaughey, U. Patel, M.B. Webb, J. Yardley, T. Andree, C. Boast, R.J. Kucharik, K. Marquis, H. Morris, R. Scerni, J.A. Moyer, Synthesis and SAR of Adatanserin: Novel Adamantyl Aryl- and Heteroarylpiperazines with Dual Serotonin 5-HT<sub>1A</sub> and 5-HT<sub>2</sub> Activity as Potential Anxiolytic and Antidepressant Agents, *J. Med. Chem.* 42 (1999) 5077–5094. doi:10.1021/jm9806704.

- [37] S.A. Savage, G.S. Jones, S. Kolotuchin, S.A. Ramrattan, T. Vu, R.E. Waltermire, Preparation of Saxagliptin, a Novel DPP-IV Inhibitor, *Org. Process Res. Dev.* 13 (2009) 1169–1176. doi:10.1021/op900226j.
- [38] Y. Dong, S. Wittlin, K. Sriraghavan, J. Chollet, S.A. Charman, W.N. Charman, C. Scheurer, H. Urwyler, J. Santo Tomas, C. Snyder, D.J. Creek, J. Morizzi, M. Koltun, H. Matile, X. Wang, M. Padmanilayam, Y. Tang, A. Dorn, R. Brun, J.L. Vennerstrom, The Structure–Activity Relationship of the Antimalarial Ozonide Arterolane (OZ277), *J. Med. Chem.* 53 (2010) 481–491. doi:10.1021/jm901473s.
- [39] A.S. Hassan, A.A. Askar, A.M. Naglah, A.A. Almhizia, A. Ragab, Discovery of New Schiff Bases Tethered Pyrazole Moiety: Design, Synthesis, Biological Evaluation, and Molecular Docking Study as Dual Targeting DHFR/DNA Gyrase Inhibitors with Immunomodulatory Activity, *Molecules.* 25 (2020). doi:10.3390/molecules25112593.
- [40] G. Verma, G. Chashoo, A. Ali, M.F. Khan, W. Akhtar, I. Ali, M. Akhtar, M.M. Alam, M. Shaquiquzzaman, Synthesis of pyrazole acrylic acid based oxadiazole and amide derivatives as antimalarial and anticancer agents, *Bioorg. Chem.* 77 (2018) 106–124. doi:https://doi.org/10.1016/j.bioorg.2018.01.007.
- [41] S. Saueressig, J. Tessmann, R. Mastelari, L.P. da Silva, J. Buss, N.V. Segatto, K.R. Beghini, B. Pacheco, C.M.P. de Pereira, T. Collares, F.K. Seixas, Synergistic effect of pyrazoles derivatives and doxorubicin in claudin-low breast cancer subtype, *Biomed. Pharmacother.* 98 (2018) 390–398. doi:https://doi.org/10.1016/j.biopha.2017.12.062.
- [42] B. Nagaraju, J. Kovvuri, C.G. Kumar, S.R. Routhu, M.A. Shareef, M. Kadagathur, P.R. Adiyala, S. Alavala, N. Nagesh, A. Kamal, Synthesis and biological evaluation of pyrazole linked benzothiazole- $\beta$ -naphthol derivatives as topoisomerase I inhibitors with DNA binding ability, *Bioorg. Med. Chem.* 27 (2019) 708–720. doi:https://doi.org/10.1016/j.bmc.2019.01.011.
- [43] J. Bronson, M. Dhar, W. Ewing, N. Lonberg, Chapter Thirty-One - To Market, To Market—2011, in: M.C.B.T.-A.R. in M.C. Desai (Ed.), *Annu. Rep. Med. Chem.*, Academic Press, 2012: pp. 499–569. doi:https://doi.org/10.1016/B978-0-12-396492-2.00031-X.
- [44] K.D. Katariya, S.R. Shah, D. Reddy, Anticancer, antimicrobial activities of quinoline based hydrazone analogues: Synthesis, characterization and molecular docking, *Bioorg.*

- Chem. 94 (2020) 103406. doi:<https://doi.org/10.1016/j.bioorg.2019.103406>.
- [45] M.A.M.S. El-Sharief, S.Y. Abbas, M.A. Zahran, Y.A. Mohamed, A. Ragab, Y.A. Ammar, New 1,3-diaryl-5-thioxo-imidazolidin-2,4-dione derivatives: Synthesis, reactions and evaluation of antibacterial and antifungal activities, *Zeitschrift Fur Naturforsch. - Sect. B J. Chem. Sci.* 71 (2016). doi:[10.1515/znb-2016-0054](https://doi.org/10.1515/znb-2016-0054).
- [46] H. Doğan, Ş.D. Doğan, M.G. Gündüz, V.S. Krishna, C. Lherbet, D. Sriram, O. Şahin, E. Sarıpinar, Discovery of hydrazone containing thiadiazoles as *Mycobacterium tuberculosis* growth and enoyl acyl carrier protein reductase (InhA) inhibitors, *Eur. J. Med. Chem.* 188 (2020) 112035. doi:<https://doi.org/10.1016/j.ejmech.2020.112035>.
- [47] M.A. Salem, A. Ragab, A. El-Khalafawy, A.H. Makhlof, A.A. Askar, Y.A. Ammar, Design, synthesis, in vitro antimicrobial evaluation and molecular docking studies of indol-2-one tagged with morpholinosulfonyl moiety as DNA gyrase inhibitors, *Bioorg. Chem.* 96 (2020) 103619. doi:<https://doi.org/10.1016/j.bioorg.2020.103619>.
- [48] Y. A. Ammar, A. M. Sh. El-Sharief, A. Belal, S. Y. Abbas, Y. A. Mohamed, A. B. M. Mehany, A. Ragab, Design, synthesis, antiproliferative activity, molecular docking and cell cycle analysis of some novel (morpholinosulfonyl) isatins with potential EGFR inhibitory activity., *Eur. J. Med. Chem.* 156 (2018) 918–932. doi:[10.1016/j.ejmech.2018.06.061](https://doi.org/10.1016/j.ejmech.2018.06.061).
- [49] M.A. Salem, A. Ragab, A.A. Askar, A. El-Khalafawy, A.H. Makhlof, One-pot synthesis and molecular docking of some new spiropyranindol-2-one derivatives as immunomodulatory agents and in vitro antimicrobial potential with DNA gyrase inhibitor, *Eur. J. Med. Chem.* 188 (2020) 111977. doi:<https://doi.org/10.1016/j.ejmech.2019.111977>.
- [50] H.F. Rizk, M.A. El-Borai, A. Ragab, S.A. Ibrahim, Design, synthesis, biological evaluation and molecular docking study based on novel fused pyrazolothiazole scaffold, *J. Iran. Chem. Soc.* (2020). doi:[10.1007/s13738-020-01944-9](https://doi.org/10.1007/s13738-020-01944-9).
- [51] Y.A. Ammar, A.A. Farag, A.M. Ali, S.A. Hessein, A.A. Askar, E.A. Fayed, D.M. Elsis, A. Ragab, Antimicrobial evaluation of thiadiazino and thiazolo quinoxaline hybrids as potential DNA gyrase inhibitors; design, synthesis, characterization and morphological studies, *Bioorg. Chem.* 99 (2020) 103841. doi:<https://doi.org/10.1016/j.bioorg.2020.103841>.

- [52] Y. A Ammar, S. AM, M. El-Sharief, M. M Ghorab, Y. A Mohamed, A. Ragab, S. Y Abbas, New imidazolidineiminothione, imidazolidin-2-one and imidazoquinoxaline derivatives: synthesis and evaluation of antibacterial and antifungal activities, *Curr. Org. Synth.* 13 (2016) 466–475.
- [53] M. Swayampakula, P.C. McDonald, M. Vallejo, E. Coyaud, S.C. Chafe, A. Westerback, G. Venkateswaran, J. Shankar, G. Gao, E.M.N. Laurent, Y. Lou, K.L. Bennewith, C.T. Supuran, I.R. Nabi, B. Raught, S. Dedhar, The interactome of metabolic enzyme carbonic anhydrase IX reveals novel roles in tumor cell migration and invadopodia/MMP14-mediated invasion, *Oncogene.* 36 (2017) 6244–6261. doi:10.1038/onc.2017.219.
- [54] R.Z. Cer, U. Mudunuri, R. Stephens, F.J. Lebeda, IC50-to-Ki: a web-based tool for converting IC50 to Ki values for inhibitors of enzyme activity and ligand binding, *Nucleic Acids Res.* 37 (2009) W441–W445. doi:10.1093/nar/gkp253.
- [55] D. Moi, A. Nocentini, A. Deplano, G. Balboni, C.T. Supuran, V. Onnis, Structure-activity relationship with pyrazoline-based aromatic sulfamates as carbonic anhydrase isoforms I, II, IX and XII inhibitors: Synthesis and biological evaluation, *Eur. J. Med. Chem.* 182 (2019) 111638. doi:https://doi.org/10.1016/j.ejmech.2019.111638.
- [56] D. Moi, A. Nocentini, A. Deplano, S.M. Osman, Z.A. AlOthman, V. Piras, G. Balboni, C.T. Supuran, V. Onnis, Appliance of the piperidinyl-hydrazidoureido linker to benzenesulfonamide compounds: Synthesis, in vitro and in silico evaluation of potent carbonic anhydrase II, IX and XII inhibitors, *Bioorg. Chem.* 98 (2020) 103728. doi:https://doi.org/10.1016/j.bioorg.2020.103728.
- [57] <https://www.rcsb.org/structure/3IAI> and <https://www.rcsb.org/structure/1JD0>; last access 14/4/2020.
- [58] V.H. Pham, T.P. Phan, D.C. Phan, B.D. Vu, Synthesis and Bioactivity of Hydrazone-Hydrazones with the 1-Adamantyl-Carbonyl Moiety, *Mol.* . 24 (2019). doi:10.3390/molecules24214000.
- [59] A.M.S. El-sharief, Y.A. Ammar, A. Belal, M.A.M.S. El-sharief, Y.A. Mohamed, A.B.M. Mehany, G.A.M. Elhag, A. Ragab, Design , synthesis , molecular docking and biological activity evaluation of some novel indole derivatives as potent anticancer active agents and apoptosis inducers, *Bioorg. Chem.* 85 (2019) 399–412. doi:10.1016/j.bioorg.2019.01.016.
- [60] Y. A. Ammar, A. M. Sh. El-Sharief, Y. A. Mohamed, A. B. M. Mehany, A. Ragab,

- Synthesis, spectral characterization and pharmacological evaluation of novel thiazole-oxoindole hybrid compounds as potent anticancer agent, *Al Azhar Bull. Sci.* 29 (2018) 25–37. doi:10.21608/ABSB.2018.33767.
- [61] E.A. Fayed, Y.A. Ammar, A. Ragab, N.A. Gohar, A.B.M. Mehany, A.M. Farrag, In vitro cytotoxic activity of thiazole-indenoquinoline hybrids as apoptotic agents, design, synthesis, physicochemical and pharmacokinetic studies, *Bioorg. Chem.* 100 (2020) 103951. doi:https://doi.org/10.1016/j.bioorg.2020.103951.
- [62] M. Güney, A. Coşkun, F. Topal, A. Daştan, İ. Gülçin, C.T. Supuran, Oxidation of cyanobenzocycloheptatrienes: Synthesis, photooxygenation reaction and carbonic anhydrase isoenzymes inhibition properties of some new benzotropone derivatives, *Bioorg. Med. Chem.* 22 (2014) 3537–3543. doi:https://doi.org/10.1016/j.bmc.2014.04.007.
- [63] S. Göksu, A. Naderi, Y. Akbaba, P. Kalın, A. Akıncioğlu, İ. Gülçin, S. Durdagi, R.E. Salmas, Carbonic anhydrase inhibitory properties of novel benzylsulfamides using molecular modeling and experimental studies, *Bioorg. Chem.* 56 (2014) 75–82. doi:https://doi.org/10.1016/j.bioorg.2014.07.009.
- [64] M. Boztaş, Y. Çetinkaya, M. Topal, İ. Gülçin, A. Menzek, E. Şahin, M. Tanc, C.T. Supuran, Synthesis and Carbonic Anhydrase Isoenzymes I, II, IX, and XII Inhibitory Effects of Dimethoxybromophenol Derivatives Incorporating Cyclopropane Moieties, *J. Med. Chem.* 58 (2015) 640–650. doi:10.1021/jm501573b.
- [65] T. Arslan, E.A. Türkoğlu, M. Şentürk, C.T. Supuran, Synthesis and carbonic anhydrase inhibitory properties of novel chalcone substituted benzenesulfonamides, *Bioorg. Med. Chem. Lett.* 26 (2016) 5867–5870. doi:https://doi.org/10.1016/j.bmcl.2016.11.017.
- [66] N. Korkmaz, O.A. Obaidi, M. Senturk, D. Astley, D. Ekinci, C.T. Supuran, Synthesis and biological activity of novel thiourea derivatives as carbonic anhydrase inhibitors, *J. Enzyme Inhib. Med. Chem.* 30 (2015) 75–80. doi:10.3109/14756366.2013.879656.
- [67] Y. Dizdaroglu, C. Albay, T. Arslan, A. Ece, E.A. Turkoglu, A. Efe, M. Senturk, C.T. Supuran, D. Ekinci, Design, synthesis and molecular modelling studies of some pyrazole derivatives as carbonic anhydrase inhibitors, *J. Enzyme Inhib. Med. Chem.* 35 (2020) 289–297. doi:10.1080/14756366.2019.1695791.
- [68] H.T. Balaydın, M. Şentürk, S. Göksu, A. Menzek, Synthesis and carbonic anhydrase

- inhibitory properties of novel bromophenols and their derivatives including natural products: Vidalol B, *Eur. J. Med. Chem.* 54 (2012) 423–428. doi:<https://doi.org/10.1016/j.ejmech.2012.05.025>.
- [69] D.H. Barich, M.T. Zell, E.J. Munson, Physicochemical Properties, Formulation, and Drug Delivery, *Drug Deliv.* (2016) 35–48. doi:[doi:10.1002/9781118833322.ch3](https://doi.org/10.1002/9781118833322.ch3).
- [70] <http://swissadme.ch/index.php>; last access 14/4/2020.
- [71] D.F. Veber, S.R. Johnson, H.-Y. Cheng, B.R. Smith, K.W. Ward, K.D. Kopple, Molecular Properties That Influence the Oral Bioavailability of Drug Candidates, *J. Med. Chem.* 45 (2002) 2615–2623. doi:[10.1021/jm020017n](https://doi.org/10.1021/jm020017n).
- [72] L. Zheng, A.A. Alhossary, C.-K. Kwoh, Y. Mu, Molecular Dynamics and Simulation, in: S. Ranganathan, M. Gribskov, K. Nakai, C.B.T.-E. of B. and C.B. Schönbach (Eds.), Academic Press, Oxford, 2019: pp. 550–566. doi:<https://doi.org/10.1016/B978-0-12-809633-8.20284-7>.
- [73] M. Berry, B. Fielding, J. Gamielien, Practical Considerations in Virtual Screening and Molecular Docking, *Emerg. Trends Comput. Biol. Bioinformatics, Syst. Biol.* (2015) 487–502. doi:[10.1016/B978-0-12-802508-6.00027-2](https://doi.org/10.1016/B978-0-12-802508-6.00027-2).
- [74] C. George Priya Doss, C. Chakraborty, V. Narayan, D. Thirumal Kumar, Chapter Ten - Computational Approaches and Resources in Single Amino Acid Substitutions Analysis Toward Clinical Research, in: R.B.T.-A. in P.C. and S.B. Donev (Ed.), Academic Press, 2014: pp. 365–423. doi:<https://doi.org/10.1016/B978-0-12-800168-4.00010-X>.
- [75] S.S. Azam, S.W. Abbasi, Molecular docking studies for the identification of novel melatonergic inhibitors for acetylserotonin-O-methyltransferase using different docking routines, *Theor. Biol. Med. Model.* 10 (2013) 63. doi:[10.1186/1742-4682-10-63](https://doi.org/10.1186/1742-4682-10-63).